Acta Crystallographica Section B
Structural Science
ISSN 0108-7681

Superspace description of trigonal and orthorhombic $A_{1+x}A_x'B_{1-x}O_3$ compounds as modulated layered structures; application to the refinement of trigonal $Sr_6Rh_5O_{15}$

Luis Elcoro,[a]* J. Manuel Perez-Mato,[a] Jacques Darriet[b] and Ahmed El Abed[c]

[a]Departamento de Física de la Materia Condensada, Facultad de Ciencias, Universidad del País Vasco, Apartado 644, Bilbao 48080, Spain, [b]Institut de Chimie de la Matiere Condensée de Bordeaux (ICMCB-CNRS), 87 Avenue du Dr A. Schweitzer, 33608 Pessac CEDEX, France, and [c]Laboratoire de Physique des Solides, Université Mohamed I, Faculté des Sciences, Oujda, Morocco

Correspondence e-mail: wmpelcel@lg.ehu.es

Received 24 October 2002
Accepted 20 January 2003

The structures of the trigonal compounds $A_{1+x}A_x'B_{1-x}O_3$ are described, to a first approximation, as a hexagonal close-packed stacking of A_3O_9 and $A_3A'O_6$ layers. However, quantitative analyses are usually performed in superspace, with the structures considered as modulated composites made of two subsystems: chains of A cations, and columns of trigonal prisms, $A'O_6$, and octahedra, BO_6. It is demonstrated that an alternative superspace description as a single modulated structure can be found in terms of the aforementioned layers, with a composition-dependent modulation parameter and discontinuous atomic domains. In this approach, these compounds fulfill layer-stacking rules analogous to those observed in other layered compounds. These rules translate into a so-called *closeness condition* for the discontinuous atomic domains in superspace; this condition is analogous to that postulated in quasicrystals. Both superspace models, the composite and the layered model, when considered without displacive modulations, can be taken as two limiting idealized paradigms and can be used as the starting point of a structure refinement. As an example, the structure of the trigonal phase $Sr_6Rh_5O_{15}$, which was previously refined as a modulated composite [Stitzer, El Abed *et al.* (2001), *J. Am. Chem. Soc.* **123**, 8790–8796], has been refined anew, with equivalent results, as a single modulated structure taking as reference the ideal layered structure. A similar superspace layer description is applied to the recently reported orthorhombic family $A_{4m+4n}A'_nB_{4m+2n}O_{12m+9n}$. This description allows the *a priori* derivation of a refineable superspace model that includes the superspace symmetry and crenel functions and is valid for the whole family. This model has been successfully applied to the refinement of the compound $Ba_{12}Co_{11}O_{33}$ [Darriet *et al.* (2002), *Chem. Mater.* **14**, 3349–3363].

1. Introduction

The hexagonal perovskite ABO_3 can be considered as a layered structure. ABO_3 can be described by the stacking of compact $[AO_3]$ layers along the **c** direction, thus creating octahedral interstices in which the B cations are located as intermediate layers (Lander, 1951). Variations in the stacking rule and/or the inclusion of modified layers in the stacking sequence lead to numerous different compounds and homologous series, which are known as intergrowth polytypoids (Darriet & Subramanian, 1995). In particular, in recent years, the existence of a series of trigonal compounds with the general formula $A_{3n+3m}A'_nB_{3m+n}O_{9m+6n}$ has been reported, and a layered model has been proposed in order to describe the

structure of these compounds in an approximate form (Darriet & Subramanian, 1995; Stitzer, Darriet & zur Loye, 2001). These compounds are formed by the stacking along **c** of mixed layers of $[A_3O_9]$ and of $[A_3A'O_6]$. The former layer is identical to the compact layers of the ideal perovskite structure, and the $[A_3A'O_6]$ layer derives from the first by the substitution of one A' atom for three O atoms (Figs. 1*a* and 1*b*, respectively). The stacking of these mixed layers creates both octahedral and prismatic sites. The B cations are located at the octahedral interstices, and the A' cations occupy the centers of the prismatic sites. The n/m value indicates the ratio between the numbers of $[A_3A'O_6]$ and $[A_3O_9]$ layers. Whether the materials have hexagonal or rhombohedral lattices depends on the n and m values. In the ideal-layer picture, where the distance between successive layers is constant, the size of the trigonal prisms is c_{2H}, twice the size of the octahedra, where c_{2H} is the c parameter of the hexagonal perovskite. All members of the family have a similar a parameter, of around 10 Å $\simeq (3)^{1/2}a_{2H}$, and a c parameter that depends on the integers n and m. In some cases, the period of the stacking sequence and consequently the c parameter can be very long, and the structures can be considered to be incommensurate. The general formula of these compounds can be expressed in an equivalent way as $A_{1+x}(A'_xB_{1-x})O_3$, with $x = n/(3m + 2n)$, so that the composition parameter x may be any number between the limits 0 and 1/2. $x = 0$ corresponds to the reference 2H hexagonal perovskite, with no trigonal prisms, while $x = 1/2$ represents the case where all the layers are of the type $[A_3A'O_6]$. Incommensurate cases correspond formally to irrational values of x and, in practice, to experimental ratios of x with large denominators (Zakhour-Nakhl, Claridge *et al.*, 2000; Zakhour-Nakhl, Weill *et al.*, 2000; Evain *et al.*, 1998).

Recently, we have demonstrated, in the case of other layered homologous series, the great efficiency of the (3 + 1)-dimensional superspace formalism (*International Tables for Crystallography*, 1992, Vol. C, p. 797) for dealing quantitatively with layered structures, both commensurate and incommensurate (Elcoro *et al.*, 2000, 2001; Boullay *et al.*, 2002). The structures are described as modulated, with the fundamental modulation being constituted by step-like atomic occupation functions that yield the necessary (occupied) atomic positions when going from one layer to the next along the stacking sequence. The deviations of the atomic positions from their ideal-layer position are then taken into account by small displacive modulations. In this picture, the average interlayer distance is the basic distance along the stacking direction to which the modulations are referred. The fact that the presence of some atoms depends on which layer is under consideration yields discontinuous atomic domains in the superspace description, as happens when describing quasicrystals. The possible higher superspace-group symmetries of the structures can be related to the two-dimensional symmetries of the layers involved and can be derived systematically. In the families investigated, the superspace-group symmetry is usually common to the whole family, and, furthermore, the superspace description of the structures is independent of the particular composition of each member of the series. Only the modulation wavevector, which is related in a predictable way to the composition, changes significantly. This fact implies a composition-dependent strain of the (3 + 1)-dimensional superspace unit cell, while the atomic domains may change their width but keep their basic features.

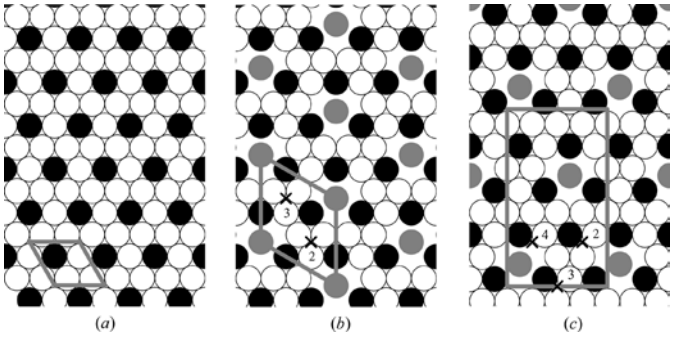

Figure 1
Schematic representations of (*a*) $[A_3O_9]$, (*b*) $[A_3A'O_6]$ and (*c*) $[A_8A'_2O_{18}]$ layers of type A. The corresponding B-type layers are obtained by inversion symmetry with respect to the origin. Black, white and gray points represent A, O and A' atoms, respectively. In (*b*) and (*c*) the crosses indicate the origins of the two and three translated layers equivalent to the layers shown in the figure for the trigonal and orthorhombic families, respectively.

The fact that we can define a common superspace structural model for all layered structures in a given family can be related to a common property of all these structures, *viz.* that the layer sequence for a given composition is the sequence that produces a distribution of the minority layers (compatible with the global composition) that is as uniform as possible, *i.e.* a so-called 'uniform' sequence. This property is translated in the superspace description into so-called *closeness conditions* among the atomic domains (analogous to the conditions used in the modeling of quasicrystals). These conditions univocally determine the essential features of the common model.

Although this superspace viewpoint of layered compounds would seem, in principle, a natural approach for the analysis of the trigonal $A_{3n+3m}A'_nB_{3m+n}O_{9m+6n}$ compounds mentioned above, the quantitative analysis, through diffraction experiments, of these structures is currently performed by a rather different approach (Ukei *et al.*, 1993; Evain *et al.*, 1998; Gourdon *et al.*, 1999; Perez-Mato *et al.*, 1999; Zakhour-Nakhl, Claridge *et al.*, 2000; Zakhour-Nakhl, Weill *et al.*, 2000; Zakhour-Nakhl, Darriet *et al.*, 2000; Stitzer, Smith *et al.*, 2001; Stitzer, El Abed *et al.*, 2001). Superspace tools are indeed employed, but the structures are considered and analyzed as commensurate or incommensurate *modulated composites* (van Smaalen, 1991). The system is considered to be modulated, with two subsystems having a different average periodicity along the c axis and the same lattice periodicity in the plane (x, y). The first subsystem is formed by the A', B and O atoms, which are seen as a set of $[A'B]O_3$ columns, parallel to the c axis, which form trigonal prisms $[A'O_6]$ and octahedra $[BO_6]$ that share faces. There are three $[A'BO_3]$ columns in the (x, y) plane of the unit cell. The second subsystem is formed by the A cations, which form three chains between the $[A'BO_3]$

columns (see Fig. 2). In this approach, the ratio n/m yields the number of trigonal prisms (N_p) and octahedra (N_o) in the chains through the expression $N_o/N_p = 1 + 3(m/n)$. In each of the three columns, the number and arrangement of the prisms and octahedra are the same, but they are shifted along the **c** direction. This viewpoint allows a simple interpretation of the diffraction diagram as coming from these two interacting subsystems, the A subsystem having a different average periodicity along the c direction from the $[A'BO_3]$ subsystem. In this modulated composite picture, each subsystem is modulated (with respect to its average periodicity) with a period corresponding to the average periodicity of the other subsystem.

The composite description of the trigonal compounds $A_{1+x}(A'_xB_{1-x})O_3$ seems quite far from the layered picture. In the composite case, two average length scales along c are defined and associated with different parts of the total structure, while in the layered case, a single average period is considered for the whole structure. In the composite description, a physical picture is somehow implicit, where the inter-subsystem interactions are much weaker than the intra-subsystem interactions. This physcial picture highlights the possible one-dimensional character of the structure. This is the situation, for instance, in typical composites such as inclusion compounds (Peral *et al.*, 2001*a*,*b*). On the other hand, in the layer description, by definition, there is not much looseness in the plane perpendicular to the stacking direction, since a significant *stiffness* of the layers is implied. Hence, we may wonder if these structures can be quantitatively described and analyzed as layered modulated structures or if only the composite description is appropriate.

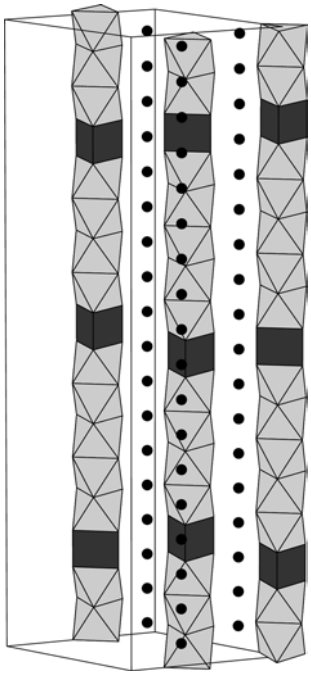

Figure 2
The idealized arrangement of octahedra and trigonal prisms for a compound with composition $x = 3/17$ viewed as a composite (octahedra/prism ratio of $N_o/N_p = 14/3$). O atoms are located at the vertices of the octahedra and prisms, and B and A' atoms occupy the centers of the octahedra and trigonal prisms, respectively. Black points represent A cations.

The purpose of this paper is to demonstrate that the trigonal $A_{1+x}(A'_xB_{1-x})O_3$ compounds can be correctly and efficiently described as modulated layered systems with a single average period, analogously to the way in which other families of layered compounds are described (Elcoro *et al.*, 2000, 2001). Starting from the usual description as composite structures, we derive a common superspace model in terms of layers and show its direct relation, as in other families, to the fact that the layer sequence for any composition should be *uniform*. Under this layer approach, the superspace group that defines the symmetry of the structures for any composition can be derived *a priori* from the symmetry of the layers, where a maximal symmetry principle is assumed. As a practical example of the efficiency of this superspace modulated-layer model, the trigonal compound $Sr_6Rh_5O_{15}$, which has been studied within the composite description (Stitzer, El Abed *et al.*, 2001), has been newly refined under the layer approach.

Finally, the power of the modulated-layer viewpoint is further demonstrated by its application to the analysis of the recently discovered (Boulahya *et al.*, 2000*a*,*b*) orthorhombic family $A_{4m+4n}A'_nB_{4m+2n}O_{12m+9n}$. These compounds also reduce to the general formula $A_{1+x}(A'_xB_{1-x})O_3$, but, in contrast with the trigonal family, they can be considered to be the result of the stacking of 'normal' compact $[A_8O_{24}]$ layers (eight units of the basic hexagonal perovskite) and layers of $[A_8A'_2O_{18}]$ composition (see Fig. 1*c*). Following analogous rules to those observed in the superspace modulated layered model of the trigonal family, a superspace model and superspace-group symmetry can be postulated for this orthorhombic family. This model has been recently applied and confirmed in the case of the $m = 2$, $n = 1$ member of the family (Darriet *et al.*, 2002).

2. Superspace model of the trigonal $A_{1+x}A_x'B_{1-x}O_3$ compounds as modulated layered structures

2.1. The modulated composite model in superspace

The superspace formalism has been extensively used in the description of different members of the trigonal family $A_{1+x}A'_xB_{1-x}O_3$, but a composite approach has always been applied (Ukei *et al.*, 1993; Evain *et al.*, 1998; Gourdon *et al.*, 1999; Perez-Mato *et al.*, 1999; Zakhour-Nakhl, Claridge *et al.*, 2000; Zakhour-Nakhl, Weill *et al.*, 2000; Zakhour-Nakhl, Darriet *et al.*, 2000; Stitzer, Smith *et al.*, 2001; Stitzer, El Abed *et al.*, 2001). The structure is interpreted as consisting of two interpenetrating substructures with the same periodicity in the (x, y) plane but with different periodicities along the c axis. The first subsystem, which is used as a reference in the superspace embedding, is the set of $[A'B]O_3$ columns along the **c** direction, which are formed, in general, by the stacking of $[BO_6]$ octahedra and $[A'O_6]$ prisms that share O_3 faces. The second subsystem is limited to the A cations, which form approximately linear chains along the **c** direction. In order to

understand this composite description, it is convenient to start from the ideal structure that corresponds to $x = 0$. For this limiting composition, the ideal structure reduces to the hexagonal perovskite 2H-$AB\mathrm{O}_3$. It is formed by the alternate stacking of two types, say A and B, of close-packed hexagonal layers with $A\mathrm{O}_3$ composition (we use the roman symbols A and B to denote the layer types and the italic symbols A and B for the general elements in the stoichiometric formula). An A layer is shown in Fig. 1(*a*), and the B layer is obtained from the A layer by the application of the inversion symmetry at the origin of the cell outlined in the figure. As a consequence of the AB packing, columns of face-sharing $[B\mathrm{O}_6]$ octahedra are formed along the c axis. The B cations are located at the centers of these octahedra. The unit-cell parameters are $a_{2H} = b_{2H} \simeq 5.7$, $c_{2H} \simeq (2/3)^{1/2} a_{2H} = 4.6$ Å and $\alpha = \beta = 90$, $\gamma = 120°$. The unit cell of this ideal structure contains a single $[B\mathrm{O}_3]$ column and a single chain of A cations. The unit cell includes along the c axis a single period of the $[B\mathrm{O}_3]$ column (containing two octahedra with different orientations) and two periods of the A chain, so that the structure can be interpreted as a commensurate composite of $[B\mathrm{O}_3]$ columns and A chains with a relation (1:2) between their periods. For a general composition $x \neq 0$, some octahedra are replaced by trigonal prisms that also share faces with the octahedra at both sides and that contain an A' cation at their center (see Fig. 2). The proportion of trigonal prisms and octahedra in the chain is the same as the proportion of A' and B cations: $x/(1 - x)$. For all compositions there are three different shifted chains so that the projection of the unit cell onto the (x, y) plane is three times the unit cell of the ideal hexagonal perovskite. The common unit-cell (x, y) projection is outlined in Fig. 1(*b*). This projection is defined by $\mathbf{a} = -\mathbf{a}_{2H} + \mathbf{b}_{2H}$, $\mathbf{b} = -\mathbf{a}_{2H} - 2\mathbf{b}_{2H}$, and contains three $[A'B]\mathrm{O}_3$ columns, which are relatively shifted by $c/3$ along the c axis. According to the stoichiometric formula, whenever a B cation is replaced in the columns by an A' cation, an extra A cation must be included in the A chains. Therefore, the average periods of the two subsystems are related by $c_1/c_2 = (1 + x)/2$, where c_1 is the average period of the $[A'B]\mathrm{O}_3$ columns (without distinguishing the cation type) and c_2 is the average period of the A chains. Taking the $[A'B]\mathrm{O}_3$ columns as the reference system in the superspace construction, the unit cell of the average structure is then formed by the basis vectors **a**, **b** (defined above) and $\mathbf{c}_1 \simeq 0.5\mathbf{c}_{2H}$. The modulation parameter of the superspace construction is the ratio between the two average periodicities, $\gamma_C = c_1/c_2 = (1 + x)/2$.

According to the experimental results, all structures of the family investigated up to now follow a common pattern in superspace. Fig. 3(*a*) depicts the (x_3, x_4) or (z, t) projection of this common superspace structural model when displacive modulations are neglected. Fig. 3(*a*) corresponds to the particular case $x \sim 1/9.1$. Four unit cells have been included to clarify the stacking sequence. In Fig. 3(*a*), a single $[A'B]\mathrm{O}_3$ column and a single chain of A cations is shown. The horizontal axis represents the z coordinate in real space (the stacking direction), and the vertical axis is parallel to the internal space. The discontinuous atomic domains (ADs) along the internal space for some atoms are introduced into the mathematical model by so-called crenel functions (Petricek *et al.*, 1995) and are represented in the figure by vertical bars. In the real structures the actual ADs deviate from the vertical position according to strong displacive modulations, which are not included in the figure. Two types of ADs, $\mathrm{O_A}$ and $\mathrm{O_B}$, which are located at $x_3 = z = 1/2$, can be distinguished for the O atoms. These types correspond to the two possible orientations of the O_3 triangles in the $[A'B]\mathrm{O}_3$ column, whose orientations are associated with the A- and B-type layers. In fact, there are three ADs of type $\mathrm{O_A}$, which represent the three O atoms at $(x, y) = (-1/6,-1/6)$, (1/6,0) and (0,1/6) that form the O_3 triangle with an A-type orienta-

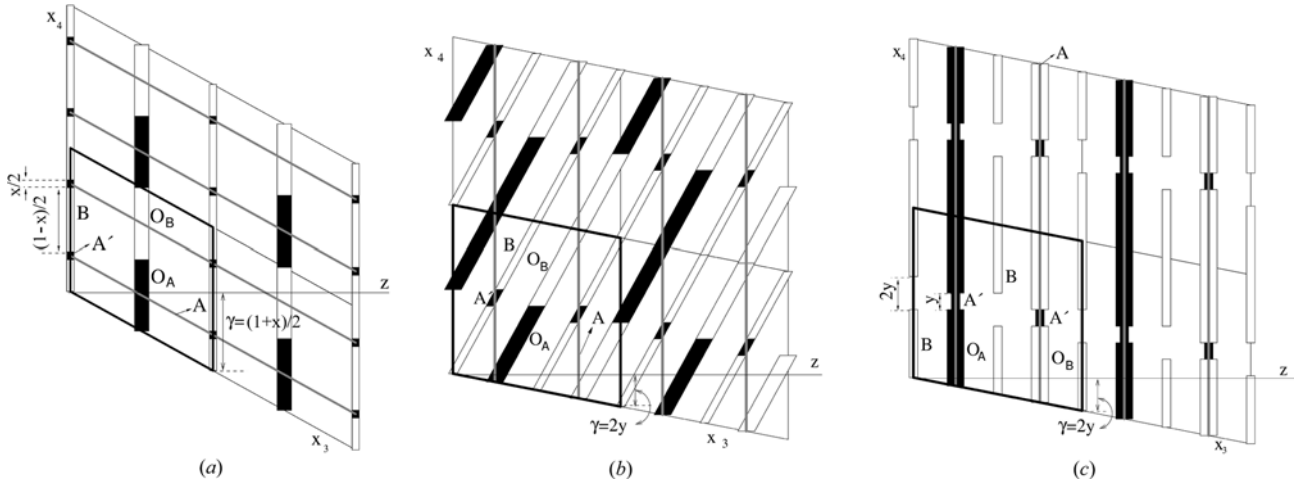

Figure 3
The superspace construction of (*a*) the ideal composite structure taking as reference the $[A'B]\mathrm{O}_3$ chains, (*b*) the ideal composite structure taking as reference the subsystem of A columns and (*c*) the ideal layer structure. (*a*) and (*b*) give rise to the same real-space atomic positions, but these differ from those of (*c*). Thick black, thick white, thin black, thin white and very thin gray atomic domains represent O atoms of A-layer type, O atoms of B-layer type, B cations, A' cations and A elements, respectively.

Table 1
Symmetry operations of the superspace groups $R\bar{3}m(00\gamma_C)0s$ (composite option) and $X\bar{3}c1(00\gamma_L)00$ [layer option, which is equivalent to $P31c(1/3, 1/3, \gamma_L)00$] and the resulting reflection conditions [superspace groups No. 160.2 and No. 163.1, respectively (*International Tables for Crystallography*, 1992, Vol. C, p. 797)].

$R\bar{3}m(00\gamma_C)0s$	$X\bar{3}c1(00\gamma_L)00$
x_1, x_2, x_3, x_4	x_1, x_2, x_3, x_4
$x_2, -x_1 + x_2, -x_3, 2\varphi_C - x_4$	$x_2, -x_1 + x_2, -x_3, 2\varphi_L - x_4$
$x_1, x_1 - x_2, x_3, \frac{1}{2} + x_4$	$x_1, x_1 - x_2, \frac{1}{2} + x_3, x_4$
$\frac{2}{3} + x_1, \frac{1}{3} + x_2, \frac{1}{3} + x_3, x_4$	$\frac{2}{3} + x_1, \frac{1}{3} + x_2, x_3, \frac{2}{3} + x_4$
$\frac{1}{3} + x_1, \frac{2}{3} + x_2, \frac{2}{3} + x_3, x_4$	$\frac{1}{3} + x_1, \frac{2}{3} + x_2, x_3, \frac{1}{3} + x_4$

Reflection conditions

$(hklm)$	$2h + k + l = 3n$	$(hklm)$	$2h + k + 2m = 3n$
$(h0lm)$	m even	$(h0lm)$	l even

tion. As the three atoms have the same z coordinate, their ADs superpose in the figure. Another three ADs of type O_B, which are located at $(x, y) = (1/6,1/6)$, $(-1/6,0)$ and $(0,-1/6)$, also superpose in this projection and generate the B-type triangles in the column. For any composition, the real structure is obtained by a horizontal cut of this superspace construction. Clearly, for the reference structure ($x = 0$), as $\gamma_C = 1/2$, the horizontal cut gives rise to alternate A- and B-type triangles, which form columns made just of octahedra. For $x \neq 0$, as $\gamma \neq 1/2$, O_A–O_A or O_B–O_B consecutive triangles enter into the sequence and introduce trigonal prisms among the octahedra in the correct proportion. To complete the construction of the columns, the A' and B cations must be considered. They are located midway between the O-atom triangles, at $x_3 = z = 0$. In Fig. 3(*a*), these ADs have been represented by thinner bars. Obviously, we must introduce the ADs that represent the B cations in the octahedral interstices, where O_A–O_B or O_B–O_A sequences occur, and the A' cations between two O_A or two O_B consecutive ADs, in the trigonal interstices. Finally, the A cations belong to the second subsystem; therefore, in the ideal-composite description they are represented by ADs parallel to the x_3 axis (van Smaalen, 1991). The other two columns and the other two A chains of an (x, y) unit cell are obtained by shifts of (1/3,2/3,2/3,0) and (2/3,1/3,1/3,0) for all the ADs represented in the figure.

Although displacive modulations have been disregarded, the structure represented in Fig. 3(*a*) is strongly modulated through the step-like occupational modulations represented by the discontinuous ADs. This scheme predicts, for any composition, the sequence of octahedra and prisms along the columns and explains the presence of the prisms as a fundamental modulation of period c_2, which is caused by the neighboring presence of the c_2 periodic A chains. We are, therefore, very far from the picture of a composite with weak interactions among the subsystems. It is, in fact, the *chemical interaction* between the two subsystems that is causing the actual location of the prisms as a primary modulation. One important feature of the configuration of ADs depicted in Fig. 3(*a*) is the fulfillment of a so-called *closeness condition* among them, so that the domain borders of neighboring ADs coincide when projected along the real z axis on the one-dimensional internal subspace. This *closeness condition* is particularly remarkable among the ADs corresponding to the A' prismatic sites, as stressed in the figure. An analogous property has been postulated for the two- or three-dimensional ADs in the superspace description of quasicrystals (Cornier-Quiquandon *et al.*, 1992; Katz & Gratias, 1993). Here, however, the property comes as an experimental fact and is directly related to the type of octahedra–prisms sequences that are realized in the columns as a function of composition. The *closeness condition* among the ADs of A' cations means that for any composition in real space, the trigonal prisms tend to separate along the columns as far as possible or, in other words, the trigonal prisms distribute along the column in the most 'uniform' way that is compatible with the discrete proportion of octahedra and prisms. The prisms can be interpreted as 'defects' in the ideal sequence of octahedra and follow a so-called 'uniform' sequence. These uniform sequences can also be directly obtained as ordered intergrowths of the simplest sequences through Farey tree rules (Perez-Mato *et al.*, 1999). According to the scheme of Fig. 3(*a*), the $[BO_6]$ octahedra and $[A'O_6]$ prisms would have the same c length (c_1). This is strongly modified when the effect of the displacive modulations is taken into account, but the *closeness condition* of the ADs, and hence also the uniform property of the sequences in the $[A'B]O_3$ columns, is maintained.

The superspace symmetry of all structures, both commensurate and incommensurate, when described in this composite approach is given by the superspace group $R\bar{3}m(00\gamma_C)0s$. A full set of symmetry operations and centering translations in the periodic basis (x_1, x_2, x_3, x_4) is given on the left side of Table 1. The parameter φ_C depends on the position along the internal space of the inversion symmetry with respect to the origin of the supercell, and φ_C is meaningful for calculating the three-dimensional real-space atomic positions according to a $t = 0$ cut. Alternatively, we can set φ_C to zero in the table and consider a non-zero t section. The corresponding reflection conditions are also included in Table 1. In the superspace description, the structural parameters are the $(x, y, z) = (x_1, x_2, x_3)$ average positions of the independent atoms in the unit cell, plus the position (x_4) of the center of the ADs and their width, if they are discontinuous. Table 2 lists these structural parameters of the composite picture. Finally, the displacive modulations of the ADs must be included to describe the real structures. These displacive modulations are, in general, restricted by the superspace site symmetry of the corresponding ADs. The general forms of the displacive modulations allowed for this family are given in the last column of Table 2. Thus, the refinement of these structures reduces to the determination of these modulation functions and the coordinates of the centers of the ADs that are not fixed by symmetry (in this case only the x_1 coordinate of the center of the oxygen AD). Once the ADs and their displacive modulations have been determined, the atomic positions are obtained by a horizontal cut of the superspace construction. For commensurate compositions, *i.e.* for rational values of the x parameter, the resulting structure is periodic. The possible space groups for these commensurate structures are quite

Table 2
Structural parameters in the superspace description for a trigonal phase of general composition $A_{1+x}(A'_xB_{1-x})O_3$ when described as a composite modulated structure [superspace group $R\bar{3}m(00\gamma_C)0s$] and as a layered structure $A(A'_yB_{1-2y})O_{3(1-y)}$ [superspace group $X3c1(00\gamma_L)00$].

The parameters of the layer option are only indicated in square brackets when they differ from those of the composite option. Underlined coordinates are refineable. The fifth and sixth columns indicate the center and size of the atomic domains. In the composite option, the B, A' and O atoms belong to the first subsystem and the A atom to the second subsystem. The A atom in the composite option is referred to its own subsystem. The seventh column shows the point symmetry of the atomic domain and the eighth column the conditions fulfilled by the corresponding displacive modulation.

Atom	x_1	x_2	x_3	x_4	Δ	Point symmetry	Displacive modulation
B	0	0	0	0	$(1-x)/2$ [$1-2y$]	$\bar{3}$	$[0, 0, U_3(x_4)] = [0, 0, -U_3(-x_4)]$
A'	0	0	0 [1/4]	1/4 [1/2]	$x/2$ [y]	32	$[0, 0, U_3(x_4)] = [0, 0, -U_3(-x_4)]$
O	1/6	0	1/2 [1/4]	1/4 [0]	1/2 [$1-y$]	12	$[U_1(x_4), U_2(x_4), U_3(x_4)] = [U_1(-x_4) - U_2(-x_4), -U_2(-x_4), -U_3(-x_4)]$
A	2/3	0	1/4	–	1	32	$[U_1(x_4), U_2(x_4), U_3(x_4)] = [U_1(-x_4) - U_2(-x_4), -U_2(-x_4), -U_3(-x_4)] \times [-U_1(x_4 - \frac{1}{3}) - U_2(x_4 - \frac{1}{3}), -U_1(x_4 - \frac{1}{3}), U_3(x_4 - \frac{1}{3})]$

limited and can be readily derived from the underlying superspace group (*International Tables for Crystallography*, 1992, Vol. C, p. 797) as a function of the modulation parameter γ_C (*i.e.* composition) and the position considered for the real-space section (φ_C in Table 1). A full list of these possible space groups, which is reproduced in Table 3, was given by Evain *et al.* (1998) and Perez-Mato *et al.* (1999). Note, however, that some of these space groups are not valid for discontinuous ADs like those presented here and can be disregarded. For more details about the superspace model of this family see Perez-Mato *et al.* (1999).

2.2. The modulated layered model in superspace

The modulated composite superspace model, as explained above, has been extensively used for the experimental determination of the structures of the trigonal family by means of diffraction techniques. However, because of the underlying ambiguity of the superspace construction, there are other possible descriptions using the superspace embedding. This fact is already evident in the case of a composite structure, where one of the two subsystems is arbitrarily taken as the reference system. The interchange of the roles of both subsystems results in a different superspace construction with a different superspace group (van Smaalen, 1991; Yamamoto, 1992). However, this situation arises for all superspace constructions. Incommensurately modulated structures and quasicrystals also infinitely accept many different (but equivalent from the physical point of view) superspace descriptions. The ambiguities of superspace construction have been discussed by Elcoro & Perez-Mato (1996). We will use the procedures described in this reference to obtain a quantitative description of the structures of this trigonal family that is in accordance with the idea that these structures come from the stacking of layers, rather than from the interpenetration of octahedra/prisms columns and atomic chains that is assumed in the composite approach.

The change from one description to the other involves two steps. In the first, the ideal (without displacive modulations) composite structure with the $[A'B]O_3$ subsystem as reference is transformed into a second superspace description of the *same ideal composite*, but taking as reference the A subsystem. Then, the ADs are continuously transformed until they form another structure, which can be interpreted as the ideal stacking of layers $[A_3O_9]$ and $[A_3A'O_6]$. This ideal layered structure can then be taken as an alternative reference over which to add displacive modulations for arriving at the actual atomic positions of the real structure. The first step essentially reduces to the interchange of the roles of the two subsystems. The construction of Fig. 3(*a*), whose structural parameters and superspace group are given in Tables 1 and 2, takes as the reference the $[A'B]O_3$ subsystem. The average unit cell is defined by the **a** and **b** cell vectors, which are common to both subsystems, and the c parameter of the $[A'B]O_3$ subsystem, c_1. The modulation parameter is the ratio between the c parameters of the second and the first subsystems, $\gamma_C = c_2/c_1$. The ADs of the A', B and O elements are vertical in the ideal model, so that the average positions of these atoms are well defined, while the A cations have no clear average position in this reference basis. The size of each AD is indicated in Fig. 3(*a*) and is fixed by the composition. To interchange the roles of the two subsystems we just construct the average unit cell with the c cell vector of the second subsystem, c_2; we take as the modulation parameter $\gamma'_L = c_1/c_2 = 1/\gamma_C$ and interchange the x_3 and x_4 coordinates in Tables 1 and 2. Finally, as is usual in the analysis of modulated structures, we keep the value of the modulation parameter in the range (0,1). When the modulation parameter falls outside this range, a new modulation parameter $\gamma_L = N \pm 1/\gamma_C$ can be defined, where N is an integer number, such that γ_L belongs to the (0,1) interval. Fig. 3(*b*) depicts the alternative superspace construction after this process, which uses the subsystem made of columns of A cations as the reference structure. In this particular case, as $x \sim 1/9.1$ and $\gamma_C \sim 0.56$, instead of using the modulation parameter $\gamma'_L = 1/\gamma_C$, the equivalent value $\gamma_L = 2 - 1/\gamma_C = 2x/(1+x) \equiv 2y \sim 0.2$ is used, where the composition-related y parameter has been introduced to simplify the notation (see below). The superspace constructions of Figs. 3(*a*) and 3(*b*) give, for the horizontal cut along **z**, the same atomic positions, so that both constructions are equivalent. The mathematical relationships between the constructions are given in *Appendix A*. Obviously, the change of the reference subsystem and modulation parameter results in a different indexing of the diffraction pattern, with different sets of main and satellite reflections. The relations between the indices of a reflection in each basis are also included in *Appendix A*.

In the second step, we transform the ADs in Fig. 3(*b*), while maintaining the same unit-cell parameters and the same widths of the atomic domains along the internal subspace. The

Table 3
Possible space groups for commensurate structures with superspace group $X\bar{3}c1(00\gamma_L)00$, modulation parameter $\gamma_L = \gamma_L = r_L/s_L$ and section φ_L (layer option) or with superspace group $R\bar{3}m(00\gamma_C)0s$, modulation parameter $\gamma_C = r_C/s_C$ and section φ_C (composite option, where r_L, s_L and s_C are integer numbers).

In all cases, the number in the *International Tables for Crystallography* (1992, Vol. C, p. 797) of the resulting space group or equivalent is given. The space groups with asterisks are not realized, as a result of the discontinuous atomic domains considered for this compound series.

r_L even	$\varphi_L = 0$ (mod. $1/s_L$)	$\varphi_L = 1/2$ (mod. $1/s_L$)	φ_L arbitrary
$s_L = 3n$	$\varphi_C = 0$ (mod. $1/s_C$)	$\varphi_C = 1/2s_C$ (mod. $1/s_C$)	φ_C arbitrary
$r_C = 3n$			
s_C even	$R\bar{3}c$ (No. 167)	*$R\bar{3}c$ (No. 167)	$R3c$ (No. 161)
r_L odd	$\varphi_L = 0$ (mod. $1/2s_L$)	$\varphi_L = 1/4s_L$ (mod. $1/2s_L$)	φ_L arbitrary
$s_L = 3n$	$\varphi_C = 0$ (mod. $1/2s_C$)	$\varphi_C = 1/4$ (mod. $1/2s_C$)	φ_C arbitrary
$r_C = 3n$			
s_C odd	*$R\bar{3}$ (No. 148)	$R32$ (No. 155)	$R3$ (No. 146)
r_L even	$\varphi_L = 0$ (mod. $1/3s_L$)	$\varphi_L = 1/2$ (mod. $1/3s_L$)	φ_L arbitrary
$s_L \neq 3n$	$\varphi_C = 0$ (mod. $1/3s_C$)	$\varphi_C = 1/2s_C$ (mod. $1/3s_C$)	φ_C arbitrary
$r_C \neq 3n$			
s_C even	$P\bar{3}c1$ (No. 165)	*$P\bar{3}c1$ (No. 165)	$P3c1$ (No. 158)
r_L odd	$\varphi_L = 0$ (mod. $1/6s_L$)	$\varphi_L = \varphi_L$ (mod. $1/6s_L$)	φ_L arbitrary
$s_L \neq 3n$	$\varphi_C = 0$ (mod. $1/6s_C$)	$\varphi_C = 1/4$ (mod. $1/6s_C$)	φ_C arbitrary
$r_C \neq 3n$			
s_C odd	*$P\bar{3}$ (No. 147)	$P321$ (No. 150)	$P3$ (No. 143)

change consists of the shearing of the oblique ADs in the figure until they are vertical, while keeping the centers of the ADs at the same positions. This transformation can also be described as the introduction within the composite model of a set of very specific sawtooth-like displacive modulation functions for the A', B and O domains. The resulting superspace model is depicted in Fig. 3(*c*). By this transformation we manage to have all the atoms in the structure with the same average periodicity. In other words, the composite model becomes, by means of a specific displacive modulation, a (atomic occupation) modulated structure with a single period. If we now take this structure as an alternative reference for the actual atomic positions of the real structure, we are describing the structure as a normal modulated structure with a single average period instead of a composite. Note that the *closeness condition* among the ADs is maintained. It is interesting to observe what happens at $z = 1/4$ or 3/4. As clearly seen in Fig. 3(*c*), at these positions there are two different intervals along the internal space. The thickest bars represent a set of three O_A atoms at $z = 1/4$ and another set of three O_B atoms at $z = 3/4$, and the thinnest bars represent A' cations located in the (x, y) plane at the center of the triangle defined by the three O atoms. With this viewpoint, we can say that the A' cation replaces the three O atoms at $z = 1/4$ or 3/4. At $z = 0$ or 1/2, whether a B cation is present depends on the internal space coordinate. It is clear from the figure that the vacancies occur whenever there is an A' cation in the previous or next AD (along z) instead of the three O atoms. Considering a horizontal cut that corresponds to the real structure, the majority motif is a sequence of three O_A atoms, a B cation, three O_B atoms, another B cation *etc.*, *i.e.* consecutive O_6 octahedra with a B cation at their center. However, in some cases, instead of the three O atoms, an A' cation is present with one B vacancy on each side. Therefore, in this region, the sequence is three O_A (O_B) atoms, an A' cation and three O_A (O_B) atoms, *i.e.* a single trigonal prism of type A or B replacing two octahedra. The z size of the trigonal prisms is now twice the size of the octahedra. Note that in the first construction (Figs. 3*a* and 3*b*) the prisms and octahedra had the same size. In addition, the A cations are now located at the same z position as the A' and O atoms, *i.e.* the A cations belong in this reference structure to a perfect layer that is perpendicular to the c axis.

The complete structure contains three $[A'B]O_3$ columns and three chains of A atoms per (x, y) unit cell, all of which in the composite construction (depicted in Fig. 3*a*) are obtained by the centering translations of Table 1. In this alternative superspace description, these centering translations become (1/3, 2/3, 0, 1/3) and (2/3, 1/3, 0, 2/3) because of the interchange of the x_3 and x_4 coordinates and the corresponding change of the modulation parameter. These symmetry elements have a non-integer component along the internal space but not along the x_3 or z coordinate. Therefore, the other two $[A'B]O_3$ columns and A chains superpose in Fig. 3(*c*) at the same z positions. As a result, a complete set of atomic surfaces is formed by three sets of ADs equivalent to the set shown in Fig. 3(*c*), with two of the sets being shifted, by 1/3 and 2/3, along x_4 with respect to that of the figure. Obviously, these two sets of additional ADs are also globally shifted by (1/3, 2/3) and (2/3, 1/3), respectively, on the (x, y) plane. As an example, Fig. 4 schematically shows the effect of the superposition of the three sets of ADs at $z = 1/4$. According to the different types of AD superpositions, the internal space is divided into different intervals. In some regions, nine O atoms and three A cations are located at the same z coordinate, and thus $[A_3O_9]$ layers are built up with the (x, y) coordinates corresponding to the ideal configuration of an A-type layer, as shown in Fig. 1(*a*). For other values of the internal coordinate, two sets of ADs contribute six O atoms and the third contributes a single A' atom. This superposition happens in three different ways, which depend on which of the three AD sets contributes the A' atom. In these cases, $[A_3A'O_6]$ layers are built up. One of these three layers is depicted in Fig. 1(*b*), and the other two are shifted by (1/3, 2/3) and (2/3, 1/3). The three layers can be denoted as A_1, A_2 and A_3 layers. Similarly, four possible B-type layers are located at $z = 3/4$: B (with $[A_3O_9]$ composition), B_1, B_2 and B_3 (with $[A_3A'O_6]$ composition). Midway between these layers, the B cations also form layers either of three atoms (located in the octahedral interstices between consecutive $[A_3O_9]$ layers) or of two atoms of three different types, midway between an $[A_3O_9]$ and an $[A_3A'O_6]$ layer, in the two resulting octahedral interstices.

Fig. 5 shows a scheme of the resulting superspace construction, which stresses the possible interpretation of the structure as being formed by the stacking of layers. The stoichiometric formula can be rewritten in terms of the parameter $y = x/(1 + x) = n/3(m + n)$ as $AA'_yB_{1-2y}O_{3(1-y)}$, which is a more natural way to indicate the atomic proportions from Fig. 5. The proportion of substituted layers $[A_3A'O_6]$ in a layer-

sequence period is given by $3y$. This formula uses the A cations, which are present in all layers at the same (x, y) positions, as the reference composition and stresses the substitution of a single A' cation for three O atoms. We have thus arrived at a zeroth-order superspace model for the description of this family. This model corresponds to a sequence of ideal layers of $[A_3O_9]$ and $[A_3A'O_6]$ that stack along the c axis, with B cations in their octahedral interstices, as proposed by Darriet & Subramanian (1995). The difference is that the present superspace model predicts a specific layer-stacking sequence for each composition and can be further refined to describe real structures, with the refinement starting from the ideal layer configuration. The superspace group and reflection conditions of this alternative superspace embedding/setting that corresponds to the layer description are given in the second column of Table 1. The structural parameters of the asymmetric unit (centers and width of the atomic domains, point symmetry, and general expressions for the displacive modulations) are given in brackets in Table 2.

2.3. Properties of the layer model: layer-stacking rules

At this point, we can consider whether it is possible to predict *a priori* the superspace construction of Fig. 5 and its superspace symmetry if we know only that the structure consists basically of the stacking of layers, as shown in Figs. 1(*a*) and 1(*b*), and equivalent sequences. Indeed, it is possible to show that the superspace layer model, which is derived above as valid for all structures of the family, implies that some general rules are being fulfilled by the layer sequences and that these rules are indeed sufficient to derive the model univocally. These general rules could then be used in other layered structural families to derive *a priori* the relevant superspace model.

Four main principles seem to be at work: (i) the alternation of layers of type A and B; (ii) the physical equivalence of layers, independently of their type (A or B) or of origin shifts; (iii) the presence in the structure of all types of substituted/modified layers that differ by origin shifts; (iv) the uniform distribution of the substituted/modified layers. In the following, we briefly schematize the use of these principles to derive the superspace modulated-layer model of the trigonal family $A_{1+x}A'_xB_{1-x}O_3$.

Firstly, as the sequence along the c direction should alternate the two types of layers (A and B), the simplest way to define the average unit cell is to take as the average c parameter the distance between two consecutive A-type layers, *i.e.* the average unit cell contains one A-type layer and one B-type layer. In the (x, y) plane, the unit cell should define a lattice compatible with the two-dimensional lattices of all layers involved in the stacking sequence. In the present case, that lattice coincides with the lattice of the substituted layers $[A_3A'O_6]$. The unit cell on the (x, y) plane is then the unit cell shown in Fig. 1(*b*). Starting from the original formulation of the compound series, $A_{3n+3m}A'_nB_{3m+n}O_{9m+6n}$, the ratio of the number of $[A_3O_9]$ and substituted $[A_3A'O_6]$ layers in the stacking sequence is m/n. This fact, translated into the superspace construction, means that the total widths of the ADs representing normal and substituted layers have the ratio m/n, which should be true for the two kinds of layers (A and B). Therefore, along the internal space, the $x_4 \in (0, 1)$ domain representing the A-type layers has to be divided to represent layers of $[A_3O_9]$ composition and three different but equivalent layers of $[A_3A'O_6]$ composition. As the last three substituted layers are equivalent, their width must be the same, and the relative location of the ADs for those layers must be *symmetric*. There is no reason to favor one of them with respect to the others. The simplest way to fulfill these requirements is realized in Fig. 5 for both A-type and B-type layers. However, these requirements would also be satisfied after the interchange or permutation of the A_i ($i = 1, 2, 3$) and/or the B_i domains. Among the five configurations for the A_i

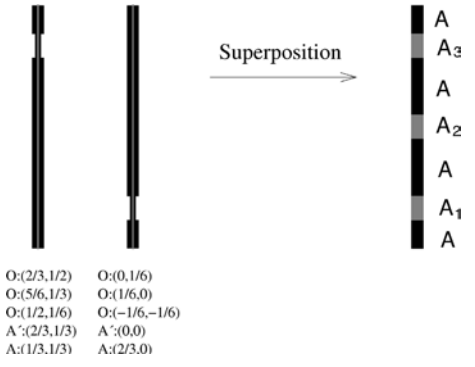

Figure 4
A scheme showing how individual atomic domains produce the layer domains in superspace. Three equivalent but translated sets of atomic domains superpose at $z = 1/4$ of Fig. 3(*c*). The superposition divides the internal space into six regions with two different compositions: $[A_3O_9]$ (A-type layer) and $[A_3A'O_6]$. In the last case, there are three different possibilities, namely the A_1, A_2 and A_3 layers. The same division occurs for the layers of type B at $z = 3/4$.

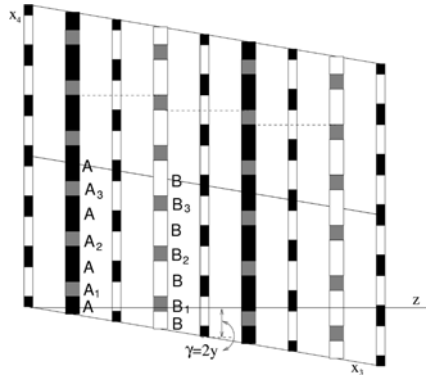

Figure 5
An alternative scheme of the layer model, with all the projected atomic domains (as indicated in Fig. 4). Thick black and white domains represent layers of type A and B of $[A_3O_9]$ composition. Thick gray domains denote A_i and B_i layers of $[A_3A'O_6]$ composition. Thin black and white domains represent layers of three and two B cations for each (x, y) unit cell, respectively. These cations are located at the corresponding octahedral interstices created by the two neighboring layers. Dotted lines help to check that the closeness condition is fulfilled (see text).

domains that differ from that of Fig. 5, two of them differ by a shift of 1/3 or 2/3 along the internal space, so that they are completely equivalent. The other three are also equivalent to the previous configurations but with the sign of the stacking direction changed. The same behavior is seen for the B_i domains. Nonetheless, if the position of the A_i domains were fixed as in Fig. 5, the interchange of the B_i domains would result in different and non-equivalent superspace constructions with different superspace groups, which would give rise to different layer-stacking sequences in real space. However, A_1 and B_1 (or A_2 and B_2; A_3 and B_3) layers must be uniformly distributed (separated as far as possible in the stacking sequence). By inspection, these conditions are only fulfilled when neighboring A_i- and B_i-layer domains satisfy the closeness condition mentioned previously, *i.e.* when the lower limit of the projection of one domain onto the internal space coincides with the upper limit of the projection of the following domain onto the internal space. This closeness condition is highlighted in Fig. 5 with dotted lines. Note that this closeness condition forces γ_L to have the known specific value of $\gamma_L = 2y = 2x/(1 + x)$. For any composition, looking at the construction of Fig. 5, it is evident that the largest distance between A_1 and B_1 layers in the horizontal real space happens when their closeness condition is fulfilled. For example, if the B_1 and B_2 atomic domains were interchanged in Fig. 5, the distance along the c axis between A_1 and B_1 (and also between A_2 and B_2 pairs) belonging to a horizontal section would be smaller than the resulting distance in Fig. 5.

Therefore, very general simple principles, mainly that of the *uniformity* of the layer sequence, are sufficient to yield the superspace model of Fig. 5 as unique (except for equivalent distributions of the ADs). The model is such that the stacking sequence realized at each composition is the sequence that distributes the $[A_3A'O_6]$ layers in the most uniform way, thus keeping a hexagonal AB stacking, with complete equivalence between the three types of $[A_3A'O_6]$ layers. It is important to see how these rules, which are implicit in the superspace construction of Fig. 5, can be applied directly to derive the layer sequence for any composition. For the simple case of an equal number of $[A_3O_9]$ and $[A_3A'O_6]$ layers ($n = m = 1$), the stacking-layer sequence will be $\langle 11\rangle_L$, *i.e.* a sequence of $1[A_3O_9]$–$1[A_3A'O_6]$ layers (the L subindex is used to differentiate these layer sequences from those of octahedra and trigonal prisms along the $[A'B]O_3$ columns). The stacking period is then obtained by repetition of this layer sequence, with the three types of $[A_3A'O_6]$ layers changed consecutively, until an actual period is attained. Thus, the stacking period is $AB_1AB_2AB_3$ or equivalently $BA_1BA_2BA_3$. Similarly, if $m = 1$ and $n = 2$, we have a sequence $\langle 12\rangle_L$ with a period of 18 layers in the pattern $AB_1A_2BA_3B_1AB_2A_3BA_1B_2AB_3A_1BA_2B_3$. In the inverse situation, for $m = 2$ and $n = 1$, the sequence of $[A_3O_9]$ and $[A_3A'O_6]$ layers is $\langle 21\rangle_L$, which yields a period of 18 layers in the form $ABA_1BAB_2ABA_3BAB_1ABA_2BAB_3$. In a more general and complex case, we can again derive the uniform layer sequence using the Farey tree for the fraction $n/(n + m)$. For instance, for $n = 3$ and $m = 5$, as $3/8 = 1/3 \oplus 1/3 \oplus 1/2$, in the sense of the Farey tree, the sequence is to be $\langle (21)^2(11)\rangle_L$: *i.e.* a sequence of two consecutive blocks that correspond to the case $n = 1$, $m = 2$ $[n/(n + m) = 1/3]$ plus a block that corresponds to $n = 1, m = 1$ $[n/(n + m) = 1/2]$. The actual layer-stacking period would then be $ABA_1BAB_2AB_3$, or equivalently $BAB_1ABA_2BA_3$, $ABA_2BAB_3AB_1$ *etc.* All the equivalent sequences are related by twinning (Gourdon *et al.*, 2001). These layer sequences yield specific octahedra–prism sequences along the $[A'B]O_3$ columns, where the distribution of prisms is also uniform. For instance, for $m = n = 1$, each column has a sequence of four octahedra to one prism $\langle 41\rangle$ that corresponds to $x = 1/5$ (one prism every five motifs). For $m = 1, n = 2$, the sequence in each column is $\langle 3121\rangle$ for a ratio of prisms $x = 2/7$ *etc.* The octahedra and prism sequences can then also be obtained using Farey tree rules, in this case for the ratio x. The prisms, the minority motif, are therefore always disjointed in the sequences.

The superspace group describing the symmetry of the ideal layer configuration given by Fig. 5 is $X\bar{3}c1(00\gamma_L)00$. This is indeed the superspace group [expressed in its equivalent form $R\bar{3}m(00\gamma_C)0s$] observed in the compounds of the family when working in the composite setting, with the $[A'B]O_3$ subsystem as the reference (see §2.2 and Table 1). Therefore, the maximal superspace symmetry defined by the ideal-layer (composition-dependent) uniform sequence is maintained in the real structures of this family, where the atoms strongly deviate from the ideal-layer positions through displacive modulations.

Similar basic principles regarding the superspace description of layered compounds and its relation to the layer-stacking rules have been shown to be valid in other composition-flexible systems (Perez-Mato *et al.*, 1999, 2003; Elcoro *et al.*, 2000, 2001; Boullay *et al.*, 2002; Darriet *et al.*, 2002). We can, therefore, talk of a very general and powerful approach for predicting the symmetry and structural properties for families of this type of compound. In cases where real structures do not maintain the maximal superspace symmetry, one of its subgroups can be identified as the working symmetry (Elcoro *et al.*, 2001).

2.4. The layers of *B* cations

The B-layer domains fill, at intermediate z coordinates, the x_4 regions that correspond to octahedral interstices between successive layers. In Fig. 5, as the number of $[A_3O_9]$ layers is larger than the number of $[A_3A'O_6]$ layers (which implies that, in the superspace construction, the total size of the domains of the $[A_3O_9]$ layers is larger than the net size of the $[A_3A'O_6]$ domains), there are two kinds of layer domains for the B cations. These domains are shown with different gray levels in Fig. 5. There are three atoms in the layer (three B ADs) when the two adjacent layers have $[A_3O_9]$ composition and two atoms (two ADs) when the consecutive layers are of $[A_3O_9]$ and $[A_3A'O_6]$ type.

It is interesting to analyze the limits of the composition, and the possibility of having new atomic layers of different compositions within the same superspace model with the same model of atomic ADs. For $y < 1/6$, there are more $[A_3O_9]$

layers than $[A_3A'O_6]$ layers, and the situation remains as depicted in Fig. 5, with the *B* ADs forming two types of *B*-cation layer domains: one with three and one with two atoms in the (x, y) unit cell. However, when $y > 1/6$, there are more $[A_3A'O_6]$ layers than $[A_3O_9]$ layers, and, as a result, the consecutive-layer pairs in the sequence are $A–B_i$ (or $B–A_i$) and $A_i–B_j$ (or $B_i–A_j$) layers, which give rise to two and one octahedral interstices per (x, y) unit cell, respectively. For those compositions, therefore, the domain layers of *B* cations have either two or one AD. For the family composition limit $y = 1/3$ ($x = 1/2$), all the atomic layers are of the A_i (B_i) type, with a single octahedral interstice in between.

3. Application: refinement of the trigonal $Sr_6Rh_5O_{15}$ compound

Up to now, all the quantitative structural analyses, in the superspace framework, of compounds belonging to the trigonal $A_{1+x}A'_xB_{1-x}O_3$ families have been performed in the composite option (Ukei *et al.*, 1993; Zakhour-Nakhl, Claridge *et al.*, 2000; Evain *et al.*, 1998; Gourdon *et al.*, 1999; Perez-Mato *et al.*, 1999, 2003; Elcoro *et al.*, 2000, 2001; Boullay *et al.*, 2002; Darriet *et al.*, 2002; Zakhour-Nakhl, Weill *et al.*, 2000; Zakhour-Nakhl, Darriet *et al.*, 2000; Stitzer, Smith *et al.*, 2001; Stitzer, El Abed *et al.*, 2001). This option is, in most cases, the natural choice that arises from the analysis of the diffraction diagram. In general, considering two subsystems with different average periods in the composite starting model can maximize the number of main reflections and minimize the set of reflections that should be considered satellites. This approach would, in principle, also minimize the magnitude of the displacive modulations that should be refined. We therefore expect that a modulated-layer description will require larger displacive modulations, which may hamper a direct refinement. In this section, our aim is to prove that, even under these circumstances, the modulated-layer description is also suitable, in *practice*, for direct refinements of experimental diffraction data. For this purpose we have refined the $Sr_6Rh_5O_{15}$ ($x = 1/5$, $y = 1/6$) trigonal phase using the *JANA*2000 program package (Petricek & Dusek, 2000). The structure of this compound was successfully determined by Stitzer, El Abed *et al.* (2001) by single-crystal X-ray diffraction. The structure refinement was performed both in the standard three-dimensional description and in (3+1) dimensions using the superspace formalism (composite option). The authors demonstrated that the results of both refinements were equivalent, but the number of refinement parameters in the (3+1)-dimensional analysis was significantly smaller (32 against the 44 parameters used in the three-dimensional refinement). We will prove that the alternative structure determination in the superspace (layer option) also gives rise to equivalent results. For our refinement, the same set of 649 ($I > 3\sigma$) X-ray reflections has been used. A detailed description of the experimental data collection is given by Stitzer, El Abed *et al.* (2001).

The ideal model of Fig. 4, with the superspace group and structural parameters given in Tables 1 and 2, was taken as a starting point. For this compound, A = Sr, $B = Rh_o$, $A' = Rh_p$, $x = 1/5$ and $y = 1/6$. The subscripts *o* and *p* denote the octahedral and prismatic Rh atoms, respectively. As a first step, the measured (*hkl*) reflections referring to the rhombohedral supercell were transformed into (*hklm*) indices, where the four indices refer to the $\mathbf{H} = h\,\mathbf{a}^* + k\,\mathbf{b}^* + l\,\mathbf{c}^* + m\,\mathbf{q}_L$ indexing, with $\mathbf{q}_L = \gamma_L\mathbf{c}^* = 1/3\mathbf{c}^*$ in this case. This transformation leads to 644 independent reflections, 220 main reflections and 424 first-order satellites. Obviously, the classification of the reflections into main reflections and satellite reflections differs from the same classification in the composite option, as the chosen average unit cell is different in both models. In successive steps of the refinement, higher harmonics of the displacive modulations and the anisotropic thermal coefficients (we use this term because the standard *displacement parameter* could be confusing in this context) were introduced. The maximum number of terms in the Fourier expansion of the displacive modulation to be included for each AD is limited by the number of atoms it represents in a commensurate modulated structure. For example, the small AD representing the prismatic $A' = Rh_p$ cation in Fig. 3(*c*), and its translation-related cations, gives rise to a single independent atom in the three-dimensional structure. Therefore, no displacive modulations are to be included in the Fourier series. For other compositions with larger supercells, as the number of independent Rh_p atoms is also larger, more terms in the Fourier series would be permitted. As a rule, the maximum number of refineable positional-displacive parameters for each AD is the number of independent atomic coordinates that result from that AD in the three-dimensional commensurate structure. For relatively small supercells, *i.e.* for compositions with simple fractional $x = r/s$ values as is the case here, the maximal number of displacive parameters is usually required to reach reasonable *R* values. Unlike the refinement in the composite option (Stitzer, El Abed *et al.*, 2001), in the layer model there is a unique subsystem, so that no **W** matrices should be included in the system description (van Smaalen, 1991). The results of the refinement are summarized in Tables 4 and 5. In Table 4, the crystallographic data and the main results are included. This table should be compared with Table 2 of Stitzer, El Abed *et al.* (2001). The resulting *R* factors are

Table 4
Crystallographic data and structure refinement for $Sr_6Rh_5O_{15}$ in the layer option.

Chemical formula	$SrRh_{5/6}O_{2.5}$ ($N = 6$)
a, c_1, c_2 (Å)	9.6517 (5), 4.3493 (1), 2.6096 (3)
q	$c_1^*/3$
V (Å^3)	350.88
Superspace group	$X\bar{3}c1(00\gamma)00$
Section	$\varphi_L = 1/4$
No. of unique reflections	644
Criterion for observed reflections	$I < 3\sigma(I)$
Refinement on	F^2
Extinction coefficient	0.057 (10)
R, wR for all reflections	0.0368, 0.0807
R, wR for 220 main reflections	0.0333, 0.0790
R, wR for 424 first-order satellites	0.0397, 0.0823
Goodness of fit on F^2	2.91
$(\Delta/\sigma)_{max}$	−0.047

Table 5
Fractional atomic average coordinates, equivalent isotropic displacement factors, and atomic positional and DWF modulation coefficients for $Sr_6Rh_5O_{15}$ in the layer option.

Modulation functions for a parameter λ of an atom ν defined in a restricted interval are given by the following: $U^{\nu}_{\lambda}(x_4) = \sum_{n=0}^{k} U^{\nu}_{\lambda,n} ortho^{\nu}_{n}(x_4)$, where the orthogonalized functions, obtained through a Schmidt orthogonalization routine, are given by

$$ortho^{\nu}_{i}(x_4) = B^{\nu}_{0} + \sum_{n=1}^{k} A^{\nu}_{n} \sin(2\pi n x_4) + \sum_{n=1}^{k} B^{\nu}_{n} \cos(2\pi n x_4),$$

with coefficients B^{ν}_{n} and A^{ν}_{n} given below. For the Sr atom, the modulation functions are Fourier series

$$U^{\nu}_{\lambda}(x_4) = U^{\nu}_{\lambda,0} + \sum_{n=1}^{k} U^{\nu}_{\lambda,sn} \sin(2\pi n x_4) + \sum_{n=1}^{k} U^{\nu}_{\lambda,cn} \cos(2\pi n x_4).$$

The superspace group is $X\bar{3}c1(00\gamma_L)00$. (*a*) Parameters defining the position, width and equivalent thermal coefficients for the atomic domains in the four-dimensional structure.† (*b*) Parameters of the displacive modulations. (*c*) Parameters of the thermal coefficients.† (*d*) Coefficients of the orthogonalized functions.

Atom	Multiplicity	x_1	x_2	x_3	x_4	Δ	U_{eq} (Å^2)
(*a*)							
Rh_o	6	0	0	0	0	2/3	0.0092 (2)
Rh_p	6	0	0	1/4	1/2	1/6	0.0134 (5)
O	18	0.1582 (5)	0	1/4	0	5/6	0.040 (3)
Sr	6	2/3	0	1/4	–	1	0.0162 (2)

(*b*)						
$U^{Rho}_{x,1} = 0$	$U^{Rho}_{y,1} = 0$	$U^{Rho}_{z,1} = 0.0892\ (2)$	$U^{Rho}_{x,2} = 0$	$U^{Rho}_{y,2} = 0$	$U^{Rho}_{z,2} = 0$
$U^{Rho}_{x,3} = 0$	$U^{Rho}_{y,3} = 0$	$U^{Rho}_{z,3} = -0.0176\ (3)$	$U^{Rho}_{x,4} = 0$	$U^{Rho}_{y,4} = 0$	$U^{Rho}_{z,4} = 0$
$U^{O}_{x,1} = 0.0005\ (3)$	$U^{O}_{y,1} = 0.0011\ (7)$	$U^{O}_{z,1} = 0.1045\ (9)$	$U^{O}_{x,2} = 0.0077\ (5)$	$U^{O}_{y,2} = 0$	$U^{O}_{z,2} = 0$
$U^{O}_{x,3} = 0$	$U^{O}_{y,3} = 0$	$U^{O}_{z,3} = -0.0176\ (3)$	$U^{O}_{x,4} = 0$	$U^{O}_{y,4} = 0$	$U^{O}_{z,4} = 0$
$U^{Sr}_{x,s1} = 0.00801\ (5)$	$U^{Sr}_{y,s1} = 0.0160\ (1)$	$U^{Sr}_{z,s1} = 0\ (2)$	$U^{Sr}_{x,c1} = 0.01388\ (9)$	$U^{Sr}_{y,c1} = 0$	$U^{Sr}_{z,c1} = 0$
$U^{Sr}_{x,s2} = 0.00275\ (7)$	$U^{Sr}_{y,s2} = 0.0055\ (1)$	$U^{Sr}_{z,s2} = 0$	$U^{Sr}_{x,c2} = -0.0048\ (1)$	$U^{Sr}_{y,c2} = 0$	$U^{Sr}_{z,c2} = 0$

(*c*)					
$U^{Rho}_{u11,0} = 0.0068\ (3)$	$U^{Rho}_{u22,0} = 0.0068\ (3)$	$U^{Rho}_{u33,0} = 0.0140\ (4)$	$U^{Rho}_{u12,0} = 0.0034\ (1)$	$U^{Rho}_{u13,0} = 0$	$U^{Rho}_{u23,0} = 0$
$U^{Rho}_{u11,1} = 0$	$U^{Rho}_{u22,1} = 0$	$U^{Rho}_{u33,1} = 0$	$U^{Rho}_{u12,1} = 0$	$U^{Rho}_{u13,1} = 0$	$U^{Rho}_{u23,1} = 0$
$U^{Rho}_{u11,2} = -0.0007\ (3)$	$U^{Rho}_{u22,2} = -0.0007\ (3)$	$U^{Rho}_{u33,2} = -0.0058\ (4)$	$U^{Rho}_{u12,2} = -0.0004\ (2)$	$U^{Rho}_{u13,2} = 0$	$U^{Rho}_{u23,2} = 0$
$U^{Rhp}_{u11,0} = 0.0084\ (6)$	$U^{Rhp}_{u22,0} = 0.0084\ (6)$	$U^{Rhp}_{u33,0} = 0.0234\ (9)$	$U^{Rhp}_{u12,0} = 0.0042\ (3)$	$U^{Rhp}_{u13,0} = 0$	$U^{Rhp}_{u23,0} = 0$
$U^{O}_{u11,0} = 0.031\ (3)$	$U^{O}_{u22,0} = 0.093\ (6)$	$U^{O}_{u33,0} = 0.016\ (2)$	$U^{O}_{u12,0} = 0.047\ (3)$	$U^{O}_{u13,0} = 0.002\ (1)$	$U^{O}_{u23,0} = 0.003\ (2)$
$U^{O}_{u11,1} = -0.001\ (2)$	$U^{O}_{u22,1} = 0$	$U^{O}_{u33,1} = 0$	$U^{O}_{u12,1} = -0.001\ (2)$	$U^{O}_{u13,1} = -0.002\ (1)$	$U^{O}_{u23,1} = 0$
$U^{O}_{u11,2} = -0.021\ (3)$	$U^{O}_{u22,2} = -0.074\ (7)$	$U^{O}_{u33,2} = -0.004\ (2)$	$U^{O}_{u12,2} = -0.037\ (4)$	$U^{O}_{u13,2} = 0.002\ (2)$	$U^{O}_{u23,2} = 0.005\ (3)$
$U^{O}_{u11,3} = -0.001\ (3)$	$U^{O}_{u22,3} = 0$	$U^{O}_{u33,3} = 0$	$U^{O}_{u12,3} = -0.001\ (3)$	$U^{O}_{u13,3} = 0.003\ (2)$	$U^{O}_{u23,3} = 0$
$U^{O}_{u11,4} = 0.008\ (4)$	$U^{O}_{u22,4} = 0.021\ (6)$	$U^{O}_{u33,4} = -0.003\ (4)$	$U^{O}_{u12,4} = 0.010\ (3)$	$U^{O}_{u13,4} = 0.001\ (2)$	$U^{O}_{u23,4} = 0.003\ (4)$
$U^{O}_{u11,0} = 0.0147\ (3)$	$U^{O}_{u22,0} = 0.0147\ (3)$	$U^{O}_{u33,0} = 0.0193\ (5)$	$U^{O}_{u12,0} = 0.0074\ (1)$	$U^{O}_{u13,0} = 0$	$U^{O}_{u23,0} = 0$
$U^{O}_{u11,s1} = 0.0025\ (3)$	$U^{O}_{u22,s1} = 0$	$U^{O}_{u33,s1} = 0$	$U^{O}_{u12,s1} = 0.0025\ (3)$	$U^{O}_{u13,s1} = 0.0086\ (3)$	$U^{O}_{u23,s1} = 0$
$U^{O}_{u11,c1} = -0.0015\ (1)$	$U^{O}_{u22,c1} = 0.0029\ (3)$	$U^{O}_{u33,c1} = 0$	$U^{O}_{u12,c1} = 0.0015\ (1)$	$U^{O}_{u13,c1} = -0.0050\ (2)$	$U^{O}_{u23,c1} = -0.0100\ (3)$
$U^{O}_{u11,s2} = -0.0022\ (4)$	$U^{O}_{u22,s2} = 0$	$U^{O}_{u33,s2} = 0$	$U^{O}_{u12,s2} = -0.0022\ (4)$	$U^{O}_{u13,s2} = -0.0039\ (4)$	$U^{O}_{u23,s2} = 0$
$U^{O}_{u11,c2} = -0.0013\ (2)$	$U^{O}_{u22,c2} = 0.0025\ (5)$	$U^{O}_{u33,c2} = 0$	$U^{O}_{u12,c2} = 0.0013\ (2)$	$U^{O}_{u13,c2} = -0.0023\ 2)$	$U^{O}_{u23,c2} = -0.0046\ (4)$
$U^{O}_{u11,s3} = 0$	$U^{O}_{u22,s3} = 0$	$U^{O}_{u33,s3} = 0$	$U^{O}_{u12,s3} = 0$	$U^{O}_{u13,s3} = 0$	$U^{O}_{u23,s3} = 0$
$U^{O}_{u11,c3} = 0.0017\ (5)$	$U^{O}_{u22,c3} = 0.0017\ (5)$	$U^{O}_{u33,c3} = 0.0021\ (5)$	$U^{O}_{u12,c3} = 0.0009\ (2)$	$U^{O}_{u13,c3} = 0$	$U^{O}_{u23,c3} = 0$

$ortho^{Rho}_{i}$	B^{Rho}_{0}	A^{Rho}_{1}	B^{Rho}_{1}	A^{Rho}_{2}	B^{Rho}_{2}	$ortho^{O}_{i}$	B^{O}_{0}	A^{O}_{1}	B^{O}_{1}	A^{O}_{2}	B^{O}_{2}
(*d*)											
$ortho^{Rho}_{0}$	1					$ortho^{O}_{0}$	1				
$ortho^{Rho}_{1}$	0	1.287				$ortho^{O}_{1}$	0	1.310			
$ortho^{Rho}_{2}$	−0.870	0	2.105			$ortho^{O}_{2}$	−0.309	0	1.620		
$ortho^{Rho}_{3}$	0	−0.558	0	1.628		$ortho^{O}_{3}$	0	−0.074	0	1.361	
$ortho^{Rho}_{4}$	2.055	0	−3.586	0	2.769	$ortho^{O}_{4}$	0.451	0	−0.864	0	1.726

† We have used the term *thermal coefficient* rather than the standard *displacement coefficient* to avoid confusion in the present context.

very similar. Table 5 shows the refined structural parameters (fractional atomic average coordinates, equivalent isotropic displacement factors, and atomic positional and thermal modulation coefficients). As stressed by Stitzer, El Abed *et al.* (2001), the space group of the three-dimensional structure is *R*32. According to Table 3, the relevant section of the superspace construction is therefore $\varphi_C = \varphi_L = 1/4$, in both the composite and the layer options. The independent atomic positions of the three-dimensional structure that results from the final refined superspace model are summarized in Table 6.

Table 6
Atomic positions of the three-dimensional model (section $\varphi_L = 1/4$, space group $R32$) that results from the superspace model of Table 5.

Atom	Site	x	y	z
Sr1	9(d)	0.5758	0	0
Sr2	9(e)	0.3520	0	0.5
$Rh1_o$	6(c)	0	0	0.9042
$Rh2_o$	6(c)	0	0	0.7085
$Rh3_p$	3(b)	0	0	0.5
O1	18(f)	0.1670	0.8096	0.8096
O2	9(d)	0.1653	0	0
O3	18(f)	0.8458	0.8550	0.6096

A comparison of Table 6 with Table 3 of Stitzer, El Abed *et al.* (2001) indicates that the final real-space structural model is essentially the same.

The preceding refinement demonstrates that two different superspace descriptions are suitable for the analysis of the trigonal $A_{1+x}A'_xB_{1-x}O_3$ compounds or, in other words, two different idealized superspace models with discrete atomic domains can be used as the starting point for a quantitative determination of the structure. It is interesting to compare both models with the help of Fig. 6, which contains valuable information about the differences between the two approximations. Fig. 6 shows the refined independent modulated ADs in the layer option (solid lines) plus the ADs of the Rh_o and O atoms of the ideal composite model (dashed lines), expressed in the layer setting (as in Fig. 3*b*), and the relevant points of these two ADs that correspond to real three-dimensional atomic positions. The atomic surface representing the Sr atom does not deviate from the vertical shape. This result is due to the zero value of the z component of the first two harmonics of the Fourier series that is compatible with the point symmetry of the AD (see the last column of Table 2). Therefore, the final shape of this AD coincides with the ideal shape in both starting approximations. The small AD representing the Rh_p atom is different in the composite (see Fig. 3*b*) and layer (see Fig. 3*c*) descriptions. However, this AD gives rise to just one independent atomic position in the three-dimensional structure (Table 6), and that point comes from the center of the atomic domain, which is the same in both ideal models. Therefore, the specific shape of this small AD has no relevance for this composition (in fact, it is not refined in any of the two options). The most important information in the figure lies in the shape of the ADs that represent the Rh_o and O atoms. Undoubtedly, the refined ADs are very much closer to the ideal shapes of the composite approximation than to the (vertical) shape of the ideal-layer model. In this case, we can state that the structure is much closer to the ideal 'composite modulated phase' than to a commensurate layered structure with perfect layers. This result could be expected from the very small modulation amplitudes refined for the O and Rh_o cations in the composite option (Stitzer, El Abed *et al.*, 2001). Even in this unfavorable case, however, the structure can be successfully refined using a layer description, as shown above. The number of parameters required for the refinement was, however, significantly larger than in the composite option. In the work of Stitzer, El Abed *et al.* (2001), where the composite approximation was used, the number of refined parameters was 32. In the refinement presented above, using the layer model, the number of parameters is 43. Another important parameter that indicates the proximity of the structure to the ideal composite model is the larger number of main reflections: 303, compared with 220 in the layer model. As, in the composite option, the deviation of the real ADs with respect to the reference ideal ADs is smaller than in the layer option, the number of terms of the harmonic expansion necessary to reproduce the correct shape is reduced. Other compounds of the family, however, have much larger modulations in the usual composite option (Zakhour-Nakhl, Darriet *et al.*, 2000) and therefore represent configurations that are more intermediate between the two idealizations (see, for instance, Fig. 7). A rough estimate of the closeness of the real structure to the two extreme ideal models can be obtained by a comparison of the average size of the octahedra and the trigonal prisms. As shown above, in the composite ideal approximation without displacive modulation they have the same size, whereas in the ideal layer model, the z length of the trigonal prisms is twice that of the octahedra. In the case of $Sr_6Rh_5O_{15}$, this average prism/octahedra z-length ratio is only 1.12, while in other compounds of the family the length ratio is 1.3 (El Abed *et al.*, 2001, 2002). Therefore, there are other compounds with configurations in clear intermediate states between the two ideal reference models. We also cannot dismiss the possibility that for certain cations the system may be even closer to the ideal layer reference than to the composite.

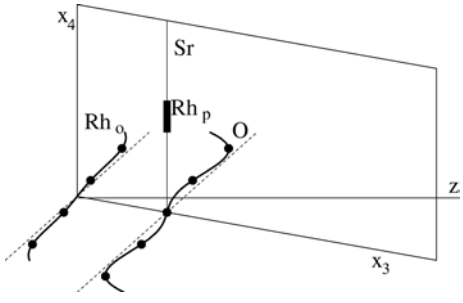

Figure 6
Independent ADs of the refined model in the layer framework (solid lines) for the trigonal $Sr_6Rh_5O_{15}$ compound. The relevant points (three-dimensional atomic positions) are also indicated for the ADs representing the Rh_o and O atoms. The ideal shapes of the Rh_o and O ADs of the composite model are indicated by dashed lines (see Fig. 3*b*).

4. Superspace description of the orthorhombic $A_{1+x}A_x'B_{1-x}O_3$ phases

Recently, also within the Ba/Co/O system, a new series of structures related to the 2H hexagonal perovskite has been discovered and a preliminary characterization by electron diffraction and electron microscopy has been reported. The members $Ba_8Co_7O_{21}$, $Ba_9Co_8O_{24}$, $Ba_{10}Co_9O_{27}$, $Ba_{11}Co_{10}O_{30}$ and $Ba_{12}Co_{11}O_{33}$ have been isolated (Boulahya *et al.*, 2000*a*,*b*). All the phases have been indexed according to an ortho-

rhombic cell. To a first approximation, they can be described as the stacking of two types of layers, as shown in Figs. 1(*a*) and 1(*c*), with compositions $[A_8O_{24}]$ (eight times the basic unit of the 2H hexagonal perovskite) and $[A_8A'_2O_{18}]$. The latter layer results from the former by an ordered removal of six O atoms that are replaced by two A' atoms (see Fig. 1*c*). The substitution can take place in four different ways, which give rise to four equivalent layers that are shifted in the (x, y) plane. The crosses in Fig. 1(*c*) indicate the origins of the other three equivalent layers. The general formula of the series can be written as $A_{4m+4n}A'_nB_{4m+2n}O_{12m+9n}$, where m/n is the proportion of $[A_8O_{24}]$ to $[A_8A'_2O_{18}]$ layers in the sequence. In the (x, y) plane, the unit-cell parameters are $a = 2a_{2H} \sim 11.4$ Å and $b = |2\mathbf{a}_{2H} + 4\mathbf{b}_{2H}| = 2(3)^{1/2}a_{2H} \sim 19.8$ Å and the c parameter depends on the composition (m and n values).

This new orthorhombic family has a very close relationship with the previously analyzed trigonal series. It can also be described as a composite system made of two subsystems: eight sets of $[A'B]O_3$ columns, made up of trigonal prisms and octahedra parallel to the c axis, separated by chains of A cations. As in the trigonal series, the A' cations occupy the prismatic sites and the B cations the centers of the octahedra. The stoichiometric formula can also be written as $A_{1+x}(A'_xB_{1-x})O_3$ with $x = n/(4m + 3n)$. For rational values of the composition parameter $x = r/s$, the integer r represents the number of octahedra and $(s - r)$ the number of trigonal prisms in the sequence of a single column. Alternatively, the stoichiometric formula can be set as $A(A'_yB_{1-2y})O_{3(1-2y)}$, with $y = x/(1 + x)$. This new parameter y represents one-fourth of the substituted layers of type $[A_8A'_2O_{18}]$ in the layer sequence of the structure, when it is described as a layered modulated phase.

The strong similarities between the two families encouraged us to investigate the existence of a superspace model for this orthorhombic case. With this purpose, we have applied the general principles outlined in §2.3 to construct the superspace model of the orthorhombic family. As the sequence along the c direction alternates the two types of layers (A and B), the average c parameter is the distance between two consecutive A-type layers. The unit cell in the (x, y) plane coincides with the lattice of the substituted layers $[A_8A'_2O_{18}]$, outlined in Fig. 1(*c*). We start from the original formulation of the compound series, $A_{4m+4n}A'_nB_{4m+2n}O_{12m+9n}$. As the ratio of the number of $[A_8O_{24}]$ and substituted $[A_8A'_2O_{18}]$ layers in the stacking sequence is m/n, the total widths of the ADs representing normal and substituted layers also have the ratio m/n. Apart from the composition of the layers, the only difference with respect to the trigonal family is the presence of four different but equivalent substituted layers. With these requirements and the closeness condition, the superspace construction in the modulated-layer model is a generalization of Fig. 5, with four A_i and four B_i domains instead of three. Fig. 8 represents an (x_3, x_4) projection of the superspace construction, where the correct widths of the ADs have been included. The modulation parameter $\gamma_L = 2y$ also coincides in the orthorhombic and trigonal series. Once the configuration of the ADs in the superspace for the ideal layer model has been obtained, the maximal superspace group is determined as the set of (3 + 1)-dimensional symmetry transformations that keeps that configuration unchanged. The superspace group is $Xdcd(00\gamma_L)qq0$, where X denotes a non-standard centering translation that is equivalent, for a different choice of the average basis, to the group $Pbnn(1/2, 1/2, \gamma_L)qq0$ listed in the *International Tables for Crystallography* (1992, Vol. C, p. 797). Table 7 lists the generators and centering translations of the superspace group, together with the resulting reflection conditions. Table 8 shows the structural parameters of the model: the average position, the center in x_4, the width of the independent atomic domains, the point symmetry and the corresponding displacive modulation according to the point symmetry. For rational compositions, the space group of the structure depends on the $\gamma_L = r_L/s_L$ ratio and the value of the φ_L phase. The full list of possible space groups is shown in Table 9. Some of these space groups are not valid for

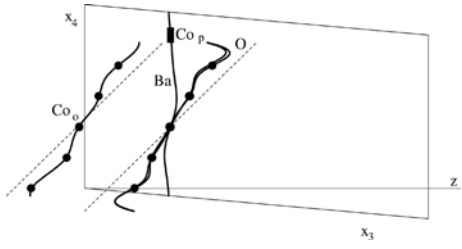

Figure 7
Independent ADs of the refined model in the layer framework (solid lines) for the orthorhombic $Ba_{12}Co_{11}O_{33}$ compound (Darriet *et al.*, 2002). The relevant points (atomic positions after cutting) are also indicated for the ADs representing the Co_o and O atoms. The ideal shapes of the Co_o and O ADs of the composite model are indicated by dashed lines (see Fig. 3).

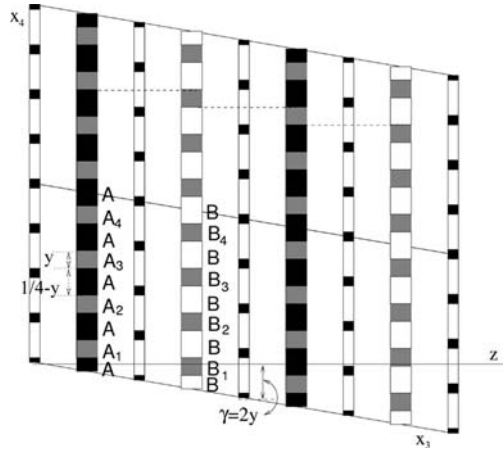

Figure 8
A scheme of the layer model for the orthorhombic family. Thick black and white domains represent layers of type A and B of $[A_8O_{24}]$ composition. Thick gray domains represents A_i and B_i layers of $[A_8A'_2O_{18}]$ composition. Thin black and white domains represent layers of eight and six B cations for each (x, y) unit cell, respectively. These cations are located at the corresponding octahedral interstices created by the two neighboring layers. Dotted lines help to check that the closeness condition is fulfilled (see the text).

Table 7
Symmetry operations of the superspace groups $Fddd(00\gamma_C)0s0$ (composite option) and $Xdcd(00\gamma_L)qq0$ (layer option) and resulting reflection conditions.

These space groups are equivalent to $Fddd(00\gamma_C)s00$ (No. 70.2) and $Pbnn(1/2, 1/2, \gamma_L)qq0$ (No. 52.7), respectively, in the *International Tables for Crystallography* (1992, Vol. C, p. 797).

$Fddd(00\gamma_C)0s0$	$Xdcd(00\gamma_L)qq0$
x_1, x_2, x_3, x_4	x_1, x_2, x_3, x_4
$-x_1, \frac{1}{4}+x_2, \frac{3}{4}+x_3, x_4$	$-x_1, \frac{1}{4}+x_2, x_3, \frac{1}{4}+x_4$
$\frac{1}{4}+x_1, -x_2, \frac{3}{4}+x_3, \frac{1}{2}+x_4$	$\frac{1}{4}+x_1, -x_2, \frac{1}{2}+x_3, \frac{1}{4}+x_4$
$\frac{1}{4}+x_1, \frac{1}{4}+x_2, -x_3, \frac{1}{2}+2\varphi_C-x_4$	$\frac{1}{4}+x_1, \frac{1}{4}+x_2, \frac{1}{2}-x_3, 2\varphi_L-x_4$
$\frac{1}{2}+x_1, \frac{1}{2}+x_2, x_3, x_4$	$\frac{1}{2}+x_1, \frac{1}{2}+x_2, x_3, x_4$
$\frac{1}{2}+x_1, x_2, \frac{1}{2}+x_3, x_4$	$\frac{1}{2}+x_1, x_2, x_3, \frac{1}{2}+x_4$
$x_1, \frac{1}{2}+x_2, \frac{1}{2}+x_3, x_4$	$x_1, \frac{1}{2}+x_2, x_3, \frac{1}{2}+x_4$
Reflection conditions	
$(hklm)$ $h+k=2n$	$(hklm)$ $h+k=2n$
$(hklm)$ $h+m=2n$	$(hklm)$ $h+l=2n$
$(0klm)$ $k+m=4n$	$(0klm)$ $k+3l=4n$
$(h0lm)$ $h+2l+m=4n$	$(h0lm)$ $h+3l+2m=4n$
$(hk00)$ $h+k=4n$	$(hk00)$ $h+k=4n$

discontinuous ADs, such as those presented here, and can be disregarded.

In the trigonal family, the superspace construction of Fig. 5 and equivalent constructions are the only constructions that fulfill the requirements of §2.3. Therefore, assuming that those principles are valid for all the compositions (as experiments have shown up to now), the solution is unique. However, this is not the case for the orthorhombic family. The simultaneous interchange of A_2 and A_3 ADs on the one hand, and of B_2 and B_3 ADs on the other (or other equivalent sets of interchanges), results in a non-equivalent superspace construction with a different superspace group that also fulfills the requirements of §2.3. In real space, the main difference between this alternative possible model and the model of Fig. 8 is the A'–A' distance between cations of successive $[A_8A'_2O_{18}]$ layers in the stacking sequence. In the model of Fig. 8, for any value of the modulation parameter in the range of validity of the y parameter, the sequence of substituted layers [independently of the type of layer (A or B)] is 1, 2, 3, 4, 1, . . . , and the A'–A' distance is the same for any two successive layers. However, for the other alternative, the sequence is 1, 3, 2, 4, 1, . . . , and there are two different A'–A' distances between successive layers: the 1–3 (2–4) distance and the 1–4 (3–2) distance. From this viewpoint, the latter alternative seems to be *less symmetric* than the former, but it cannot be discarded *a priori*. The superspace group is $X'112_1/a(00\gamma_L)$, where the symbol X' represents the non-standard centering translations (0,0,0,0), (1/4,3/4,0,1/2), (3/4,1/4,0,1/2) and (1/2,1/2,0,0). The reflection conditions for this superspace group are different from the reflection conditions of Table 7. Consequently, an X-ray or electronic diffraction experiment can elucidate which model (if either) is correct. Darriet *et al.* (2002) reported the structure determination based on single-crystal X-ray diffraction of the $Ba_{12}Co_{11}O_{33}$ ($x = 1/11$, $y = 1/12$) compound. The diffraction data fulfill the reflection conditions of Table 7 and are incompatible with the alternative superspace model, which can therefore be discarded. Therefore, as a starting point for the refinements, the model of Fig. 8, and Tables 7 and 8 was used. The successful results of the refinements (Darriet *et al.*, 2002) indicate the correctness of the model and the suitability of the superspace framework in the analysis of layered structures.

Once the distribution of the ADs in the superspace has been obtained, the layer-stacking sequence for any composition can be easily deduced. In this way, according to Fig. 8 , the layer-stacking sequence for the compound $Ba_8Co_7O_{21}$ ($x = 1/7$) is $AB_1AB_2AB_3AB_4$, which is the same as the sequence proposed in the preliminary work of Boulahya *et al.* (2000*a*,*b*). However, for $Ba_{10}Co_9O_{27}$ ($x = 1/9$), $Ba_{11}Co_{10}O_{30}$ ($x = 1/10$) and $Ba_{12}Co_{11}O_{33}$ ($x = 1/11$) compounds, the layer-stacking sequences predicted by the model above are $AB_1AB_2ABA_3BA_4B$, $AB_1ABA_2BA_3BAB_4ABA_1BAB_2AB_3$-$ABA_4B$ and $AB_1ABA_2BAB_3ABA_4B$ (or equivalents), respectively, which are at variance with the stacking sequences proposed by Boulahya *et al.* (2000*a*,*b*) for those compounds. These sequences are incompatible with our model and correspond to a less uniform distribution of the minority motifs in the structures. The quantitative analysis of the $Ba_{12}Co_{11}O_{33}$ compound (Darriet *et al.*, 2002) undoubtedly indicates that, at least in this case, the superspace construction of Fig. 8 (and its predicted layer-stacking sequence) is correct.

Finally, as in the trigonal case, a composite modulated picture of the structure is also possible. To obtain the set of ADs, superspace group and structural parameters, the procedure of §2.3 must be applied in the opposite way. The results are included in Tables 7–9. Both descriptions have been used by Darriet *et al.* (2002) as the starting point of the refinements to demonstrate that both descriptions are equally efficient and lead to the same three-dimensional structure. Fig. 7 depicts the independent atomic positions in the refined orthorhombic compound $Ba_{12}Co_{11}O_{33}$ (Darriet *et al.*, 2002), together with the ideal ADs in the composite option, referred to the average cell of the layer model. The structure, in this case, is clearly a state more intermediate between the ideal composite model and the ideal layer configuration than the state in Fig. 6, although the structure is also closer to the ideal composite. The number of parameters required in order to obtain similar R factors is, however, significantly smaller than in the previous case: 123 and 151 in the composite and the layer options, respectively (Darriet *et al.*, 2002).

5. Conclusions

As a result of the implicit arbitrariness that exists in the superspace construction of a quasiperiodic structure with discrete atomic domains, the structure of the trigonal family of compounds $A_{1+x}A'_xB_{1-x}O_3$ can be analyzed in the superspace either as a modulated composite or as a layered modulated structure. In the first case, the structure is viewed as consisting of two subsystems of different periodicity along the c axis: (i) rows of A cations and (ii) columns of face-sharing $[A'B]O_6$ trigonal prisms and octahedra. In the second case, the struc-

Table 8
Structural parameters in the superspace description for an orthorhombic phase of general composition $A(A'_yB_{1-2y})O_{3(1-y)}$ with superspace group $Xdcd(00\gamma_L)qq0$ when described as a layered structure and as a composite modulated structure $A_{1+x}(A'_xB_{1-x})O_3$[superspace group $Fddd(oo\gamma_C)0s0$].

The parameters of the composite option are only indicated (in square brackets) when they differ from those of the layer option. Underlined coordinates are refineable. The fifth and sixth columns indicate the center and size of the atomic domains. In the composite option, the B, A' and O atoms belong to the first subsystem and the A atom to the second subsystem, [$W_1 = (10|01)$ and $W_2 = (01|10)$, respectively (van Smaalen, 1991)]. The A atom in the composite option is referred to its own subsystem. The seventh column shows the point symmetry of the atomic surface and the eighth column the corresponding displacive modulations. s, a and no superscript denote a symmetric, antisymmetric and general function, respectively.

Atom	x_1	x_2	x_3	x_4	Δ	Point symmetry	Displacive modulation
B	$\underline{-1/8}$	$-1/8$	0	3/8	$1-2y$	211	$[U_1^s(x_4), U_2^a(x_4), U_3^a(x_4)]$
A'	$-1/8$	$\underline{-1/8}$	[−3/8] 1/4	[0] −1/8	[(1 − x)/2] y	121	$[U_1^a(x_4), U_2^s(x_4), U_3^a(x_4)]$
O1	$-1/8$	$\underline{-1/24}$	[−3/8] 1/4	[1/4] 3/8	[x/2] $1-y$	121	$[U_1^a(x_4), U_2^s(x_4), U_3^a(x_4)]$
O2	$\underline{-1/4}$	$\underline{-1/6}$	[1/8] $\underline{1/4}$	[1/4] 3/8	[1/2] $1-y$	1	$[U_1(x_4), U_2(x_4), U_3(x_4)]$
A	$-1/8$	$\underline{-7/24}$	$\underline{[1/8]}$ $\underline{1/4}$	[1/4] –	[1/2] 1	121	$[U_1^a(x_4), U_2^s(x_4), U_3^a(x_4)]$

ture is interpreted as the stacking of $[A_3O_9]$ and $[A_3A'O_6]$ layers along the c axis, the B cations being located in the octahedral interstices between neighboring layers. The number of prisms and octahedra in the first description, or the number of $[A_3O_9]$ and $[A_3A'O_6]$ layers in the second, is composition dependent. The change from one description to the other can be easily carried out in the superspace formalism. In fact, either of the two idealized starting models (without displacive but with occupational step-like modulations) can be described in the superspace framework of the other model, by means of specific linear (sawtooth-like) displacive modulations. A real structure deviates from both idealized paradigms, and either of them can be used as references and the starting point of a quantitative refinement, where the displacive modulations are determined. Up to now, all the structure refinements have been made with the composite option. After the demonstration of the equivalence of both approaches, we have refined the trigonal $Sr_6Rh_5O_{15}$ phase with the layer option. The atomic positions obtained are completely equivalent to those obtained by Stitzer, El Abed *et al.* (2001) with the composite option. Even in this particular case, where the results clearly indicate that the true structure is much closer to the composite-ideal model than to the ideal-layer model, the refinement has been successful.

The description in superspace of these compounds as a single modulated structure with a layered configuration, instead of the usual composite description, demonstrates that these compounds fulfill layer-stacking rules analogous to those observed in other families of layered compounds. These stacking rules translate into very simple topological properties

Table 9
Possible space groups for commensurate structures with superspace group $Xdcd(00\gamma_L)qq0$, modulation parameter $\gamma_L = r_L/s_L$ and section φ_L (layer option) or superspace group $Fddd(00\gamma_C)0s0$, modulation parameter $\gamma_C = r_C/s_C$ and section φ_C (composite option).

In all cases, the number in *International Tables for Crystallography* (1992, Vol. C, p. 797) of the resulting space group or equivalent is given. The space groups with asterisks are not realized, as a result of the discontinuous atomic domains considered for this compound series.

$s_L = 4n$, $r_C = 4n$	$\varphi_L = 0$ (mod. $1/2s_L$) $\varphi_C = 0$ (mod. $1/2s_C$) $^*F2/d11$ (No. 15)	$\varphi_L = 1/4s_L$ (mod. $1/2s_L$) $\varphi_C = 1/4$ (mod. $1/2s_C$) $Fd2d$ (No. 43)	φ_L arbitrary φ_C arbitrary $Fd11$ (No. 9)
$s_L = 4n+2$, $r_C = 4n+2$	$\varphi_L = 0$ (mod. $1/2s_L$) $\varphi_C = 0$ (mod. $1/2s_C$) $F12/d1$ (No. 15)	$\varphi_L = 1/8$ (mod. $1/2s_L$) $\varphi_C = 1/4$ (mod. $1/2s_C$) $^*F2dd$ (No. 43)	φ_L arbitrary φ_C arbitrary $F1d1$ (No. 9)
s_L odd, r_C odd	$\varphi_L = 0$ (mod. $1/4s_L$) $\varphi_C = 0$ (mod. $1/4s_C$) $C112_1/d$ (No. 14)	$\varphi_L = 1/8$ (mod. $1/4s_L$) $\varphi_C = 1/8s_C$ (mod. $1/4s_C$) $^*C222_1$ (No. 20)	φ_L arbitrary φ_C arbitrary $C112_1$ (No. 4)

to be fulfilled by the configuration of the discrete atomic domains (crenel functions) in superspace. This fact, together with the symmetry of the ideal layers, allows us to predict the starting model to be refined, including the superspace-symmetry group and set of crenel functions. We have applied this approach to the recently reported orthorhombic family $A_{4m+4n}A'_nB_{4m+2n}O_{12m+9n}$, where other types of layers exist, to derive *a priori* a refineable superspace model that is common to the whole family and can then be readily transformed into a composite description. This model has been successfully applied to the refinement of the compound $Ba_{12}Co_{11}O_{33}$ (Darriet *et al.*, 2002).

APPENDIX *A*
Mathematical relationships

In this section we summarize the mathematical relationships between the parameters in the composite and layer models. These superspace models are built up from different initial average lattices, which implies different values for the coordinates of the independent atomic surfaces, different expressions for the symmetry elements and different indexing of the diffraction patterns of the structures. In general, the set of Bragg reflections in the diffraction pattern of a modulated structure can be indexed by means of d reciprocal unit vectors $\{\mathbf{a}_i^*\}$, where $\mathbf{a}_1^*$, $\mathbf{a}_2^*$ and $\mathbf{a}_3^*$ define the reciprocal vectors of the average unit cell and the remaining $(d-3)$ elements are the independent modulation vectors. Any reflection of the diffraction pattern can be expressed as

$$\mathbf{H} = \sum_{i=1}^{d} l_i \mathbf{a}_i^*. \tag{1}$$

If a different basis, $\mathbf{a}'^*_i = \sum_{j=1}^{d} M_{ij}\mathbf{a}_j^*$, is used to index the same set of reflections, the integer indices in the new basis are related to the indices in the former basis by

$$l'_i = M^{-1}_{ji} l_j \quad or \quad \mathbf{l}' = (\mathbf{M}^{-1})^T \mathbf{l}, \tag{2}$$

where

$$\mathbf{l} \equiv (l_1, l_2, \ldots, l_d), \quad \mathbf{l}' \equiv (l_1', l_2', \ldots, l_d').$$

The new coordinates of a point in the superspace are also related to the superspace coordinates in the previous embedding through

$$x_i' = M_{ij} x_j \quad \text{or} \quad \mathbf{x}' = \mathbf{M}\mathbf{x}, \tag{3}$$

where

$$\mathbf{x}' \equiv (x_1', x_2', \ldots, x_d'), \quad \mathbf{x} \equiv (x_1, x_2, \ldots, x_d).$$

Finally, the relationship between the symmetry elements in the two constructions is

$$\{\mathbf{R}'|\mathbf{t}'\} = \mathbf{M}\{\mathbf{R}|\mathbf{t}\}\mathbf{M}^{-1} = \{\mathbf{M}\mathbf{R}\mathbf{M}^{-1}|\mathbf{M}\mathbf{t}\}, \tag{4}$$

where $\mathbf{R}$ and $\mathbf{R}'$ are the $d \times d$ matrices of the rotational parts of the symmetry elements and $\mathbf{t} \equiv (t_1, t_2, \ldots, t_d)$ and $\mathbf{t}' \equiv (t_1', t_2', \ldots, t_d')$ are the associated translations. In our particular trigonal and orthorhombic systems, the $\mathbf{a}_1 = \mathbf{a}$ and $\mathbf{a}_2 = \mathbf{b}$ unit-cell vectors are common to the composite and layer descriptions and the modulation is parallel to $\mathbf{a}_3^*$, so that the changes take place just in the (x_3, x_4) subspace. Therefore, in the reciprocal space, for every reflection in the diffraction pattern only the z component of the diffraction vector changes from one description to the other. Consequently, the matrices that relate the parameters of both models in direct and reciprocal spaces are the direct sum of the (2×2)-dimensional identity matrix and a 2×2 matrix. To simplify the notation in the following, we will write just the relations between the x_3 and x_4 coordinates in the direct space and the z components of the diffraction vector. In the composite option, the structure is interpreted as comprising two subsystems with periodicity c_1 and c_2, respectively, along the $\mathbf{z}$ direction. Taking the c_1 distance as the average unit, the $\mathbf{z}$ component of the diffraction vectors can be set as

$$H_z = l_C c_1^* + m_C q_C, \quad q_C = c_2^* = \gamma_C c_1^*, \tag{5}$$

where the C subscript denotes the composite option and the modulation parameter is related to the composition through the relation $\gamma_C = (1 + x)/2$. In §2, in order to transform from the composite to the layer option, we interchanged the x_3 and x_4 coordinates and introduced an integer, N, to keep the modulation parameter in the layer model, γ_L, in the range $(0, 1)$. Hence, the new basis for the diffraction pattern is

$$H_z = l_L c_2^* + m_L q_L, \quad q_L = N c_2^* \pm c_1^* \equiv \gamma_L c_2^*, \tag{6}$$

with

$$\begin{pmatrix} l_L \\ m_L \end{pmatrix} = \begin{pmatrix} \mp N & 1 \\ \pm 1 & 0 \end{pmatrix} \begin{pmatrix} l_C \\ m_C \end{pmatrix}. \tag{7}$$

In the direct space, the relations become

$$\begin{pmatrix} x_{3L} \\ x_{4L} \end{pmatrix} \equiv \mathbf{M} \begin{pmatrix} x_{3C} \\ x_{4C} \end{pmatrix}, \tag{8}$$

with

$$\mathbf{M} \equiv \begin{pmatrix} 0 & 1 \\ \pm 1 & N \end{pmatrix}.$$

Then, the symmetry elements are related by

$$\{\mathbf{R}_{34L}|\mathbf{t}_{3L}, \mathbf{t}_{4L}\} = \mathbf{M}\{\mathbf{R}_{34C}|\mathbf{t}_{3C}, \mathbf{t}_{4C}\}M^{-1}, \tag{9}$$

where $\mathbf{R}_{34C}$ and $\mathbf{R}_{34L}$ are the 2×2 matrices of the symmetry elements that act on the (x_3, x_4) subspace in the composite and layer models, respectively, and $\mathbf{t}_3$ and $\mathbf{t}_4$ are the associated translation components. As $\mathbf{R}_{34C} = \pm$Identity,

$$\mathbf{R}_{34L} = \mathbf{R}_{34C}, \qquad \begin{pmatrix} \mathbf{t}_{3L} \\ \mathbf{t}_{4L} \end{pmatrix} = \mathbf{M} \begin{pmatrix} \mathbf{t}_{3C} \\ \mathbf{t}_{4C} \end{pmatrix}. \tag{10}$$

In the trigonal and orthorhombic phases analyzed above, for the composition range $x \in (0, 1/2)$, the minus sign in (6) is the relevant sign and $N = 2$. In this case, the change through the $\mathbf{M}$ matrix is equivalent to taking the second subsystem as the reference and introducing a

$$\mathbf{W} \equiv \begin{pmatrix} -1 & 2 \\ 0 & 1 \end{pmatrix} \tag{11}$$

matrix (van Smaalen, 1991) for the first subsystem, thus hiding the layer picture of the structure. The expressions above have been used to create Tables 1 and 2 for the trigonal family and Tables 7 and 8 for the orthorhombic family.

This work has been supported by the DGESIC (Project No. PB98-0244) and the UPV (Project No. 9/UPV 00063.310–13564/2001). We gratefully thank Vaclav Petricek for valuable comments and help using *JANA*.

References

Boulahya, K., Parras, M. & Gonzalez-Calbet, J. M. (2000*a*). *Chem. Mater.* **12**, 2727–2735.
Boulahya, K., Parras, M. & Gonzalez-Calbet, J. M. (2000*b*). *J. Solid State Chem.* **151**, 77–84.
Boullay, Ph., Trolliard, G., Mercurio, D., Perez-Mato, J. M. & Elcoro, L. (2002). *J. Solid State Chem.* **164**, 261–271.
Cornier-Quiquandon, M., Gratias, D. & Katz, A. (1992). *Methods of Structural Analysis of Modulated Structures and Quasicrystals*, edited by J. M. Perez-Mato, F. J. Zuniga & G. Madariaga, pp. 313–332. Singapore: World Scientific.
Darriet, J., Elcoro, L., El Abed, A. & Perez-Mato, J. M. (2002). *Chem. Mater.* **14**, 3349–3363.
Darriet, J. & Subramanian, M. A. (1995). *J. Mater. Chem.* **5**, 543–552.
El Abed, A., Gaudin, E. & Darriet, J. (2002). *Acta Cryst.* C**58**, i138–i140.
El Abed, A., Gaudin, E., Lemaux, S. & Darriet, J. (2001). *Solid State Sci.* **3**, 887–897.
Elcoro, L. & Perez-Mato, J. M. (1996). *Phys. Rev.* B**54**, 12115–12124.
Elcoro, L., Perez-Mato, J. M. & Withers, R. (2000). *Z. Kristallogr.* **215**, 727–739.
Elcoro, L., Perez-Mato, J. M. & Withers, R. L. (2001). *Acta Cryst.* B**57**, 471–484.
Evain, M., Boucher, F., Gourdon, O., Petricek, V., Dusek, M. & Bezdicka, P. (1998). *Chem. Mater.* **10**, 3068–3076.
Gourdon, O., Cario, L., Petricek, V., Perez-Mato, J. M. & Evain, M. (2001). *Z. Kristallogr.* **216**, 541–555.
Gourdon, O., Petricek, V., Dusek, M., Bedzdicka, P., Durovic, S., Gyepesova, D. & Evain, M. (1999). *Acta Cryst.* B**55**, 841–848.
Katz, A. & Gratias, D. (1993). *J. Non-Cryst. Solids*, **153/154**, 187–195.
Lander, J. (1951). *Acta Cryst.* **4**, 148–156.

Peral, I., Madariaga, G., Petricek, V. & Breczewski, T. (2001*a*). *Acta Cryst.* B**57**, 378–385.
Peral, I., Madariaga, G., Petricek, V. & Breczewski, T. (2001*b*). *Acta Cryst.* B**57**, 386–393.
Perez-Mato, J. M., Etrillard, J., Kiat, J. M., Liang, B. & Ling, C. T. (2003). In preparation.
Perez-Mato, J. M., Zakhour-Nakhl, M., Weill, F. & Darriet, J. (1999). *J. Mater. Chem.* **9**, 2795–2808.
Petricek, V. & Dusek, M. (2000). *JANA*2000. Institute of Physics, Czech Academy of Sciences, Prague, Czech Republic.
Petricek, V., van der Lee, A. & Evain, M. (1995). *Acta Cryst.* A**51**, 529–535.
Smaalen, S. van (1991). *Phys. Rev. B*, **43**, 11330–11341.
Stitzer, K. E., Darriet, J. & zur Loye, H. C. (2001). *Solid State Mater. Sci.* **5**, 535–544.
Stitzer, K. E., El Abed, A., Darriet, J. & zur Loye, H. C. (2001). *J. Am. Chem. Soc.* **123**, 8790–8796.
Stitzer, K. E., Smith, M. D., Darriet, J. & zur Loye, H. C. (2001). *Chem. Commun.* **17**, 1680–1681.
Ukei, K., Yamamoto, A., Watanabe, Y., Shishido, T. & Fukuda, T. (1993). *Acta Cryst.* B**49**, 67–72.
Yamamoto, A. (1992). *Acta Cryst.* A**48**, 476–483.
Zakhour-Nakhl, M., Claridge, J. B., Darriet, J., Weill, F., zur Loye, H. C. & Perez-Mato, J. M. (2000). *J. Am. Chem. Soc.* **122**, 1618–1623.
Zakhour-Nakhl, M., Darriet, J., Claridge, J. B., zur Loye, H. C. & Perez-Mato, J. M. (2000). *Int. J. Inorg. Mater.* **2**, 503–512.
Zakhour-Nakhl, M., Weill, F., Darriet, J. & Perez-Mato, J. M. (2000). *Int. J. Inorg. Mater.* **2**, 71–79.